Fig. 2. FPLCA in this family results from the mutation p.G723V in the oncostatin M receptor β. (a) A heterozygous nucleotide substitution, c.2168G > T (NM_003999) in the *OSMR* gene is present in the proband and her mother. (b) The mutation abolishes a restriction enzyme cut site for *Nla*IV, resulting in an undigested DNA band in affected individuals. M, marker; U, control (undigested); C, control (digested); P, proband; M, proband's mother. (Digested PCR product spans exon 15 and flanking introns of *OSMR*.) (c) The mutation p.G723V is located within the FNIII-like domain region, similarly to the previous reported mutations, p.G618A and p.I691T. CBD, cytokine binding domain; FNIII, fibronectin type III-like domain; tm, transmembranous domain; cp, cytoplasmic domain.

OSMRβ were upregulated in psoriatic and atopic skin, suggesting that OSM is a potent activator of skin inflammation [7]. As to PLCA, the histopathological finding of inflammation is less obvious, and main histological features are the pigmentary incontinence and amyloids in the papillary dermis suggesting the apoptosis of basal keratinocytes. Jak/STAT, Erk1/2 and PI3K/Akt signaling, which is downstream of IL-6 type cytokine signaling, have been reported to have antiapoptotic effects in several tumor cell lines [10,11]. These findings suggest the functional decrease of IL-6 type cytokine receptor (including OSMRβ) may lead to a condition that is more susceptible to apoptosis. Recently, diminished innervations of epidermis and dermoepidermal junction were identified in PLCA skin, indicating the damage to the nerve fibers as a possible explanation for the severe pruritis [12]. It is speculated that the pruritis may be the result of hypersensitivity of the remaining nerve fibers as a response to the neurodegeneration [12]. OSMRβ is also expressed in afferent nerve fibers in the spinal cord and the dermis of the skin [13]; therefore, the pathophysiology of PLCA may involve both cutaneous and neural components.

Although FPLCA is relatively common in Asian countries, our case represents the first *OSMR* mutation to be reported in Japanese population.

References

[1] Kumakiri M, Hashimoto K. Histogenesis of primary localized cutaneous amyloidosis: sequential change of epidermal keratinocytes to amyloid via filamentous degeneration. J Invest Dermatol 1979;73:150–62.

[2] Kobayashi H, Hashimoto K. Amyloidogenesis in organ-limited cutaneous amyloidosis: an antigenic identity between epidermal keratin and skin amyloid. J Invest Dermatol 1983;80:66–72.

[3] Arita K, South AP, Hans-Filho G, Sakuma TH, Lai-Cheong J, Clements S, et al. Oncostatin M receptor-beta mutations underlie familial primary localized cutaneous amyloidosis. Am J Hum Genet 2008;82:73–80.

[4] Heinrich PC, Behrmann I, Haan S, Hermanns HM, Muller-Newen G, Schaper F. Principles of interleukin (IL)-6-type cytokine signalling and its regulation. Biochem J 2003;374:1–20.

[5] Dillon SR, Sprecher C, Hammond A, Bilsborough J, Rosenfeld-Franklin M, Presnell SR, et al. Interleukin 31, a cytokine produced by activated T cells, induces dermatitis in mice. Nat Immunol 2004;5:752–60.

[6] Finelt N, Gazel A, Gorelick S, Blumenberg M. Transcriptional responses of human epidermal keratinocytes to oncostatin-M. Cytokine 2005;31:305–13.

[7] Boniface K, Diveu C, Morel F, Pedretti N, Froger J, Ravon E, et al. Oncostatin M secreted by skin infiltrating T lymphocytes is a potent keratinocyte activator involved in skin inflammation. J Immunol 2007;178:4615–22.

[8] Kurth I, Horsten U, Pflanz S, Timmermann A, Kuster A, Dahmen H, et al. Importance of the membrane-proximal extracellular domains for activation of the signal transducer glycoprotein 130. J Immunol 2000;164:273–82.

[9] Timmermann A, Küster A, Kurth I, Heinrich PC, Müller-Newen G. A functional role of the membrane-proximal extracellular domains of the signal transducer gp130 in heterodimerization with the leukemia inhibitory factor receptor. Eur J Biochem 2002;269:2716–26.

[10] Chen RH, Chang MC, Su YH, Tsai YH, Kuo ML. Interleukin-6 inhibits transforming growth factor beta-induced apoptosis through the phosphatidylinositol 3-kinase/Akt and signal transducers and activators of transcription 3 pathways. J Biol Chem 1999;274:23013–9.

[11] Mirmohammadsadegh A, Mota R, Gustrau A, Hassan M, Nambiar S, Marini A, et al. ERK1/2 is highly phosphorylated in melanoma metastases and protects melanoma cells from cisplatin-mediated apoptosis. J Invest Dermatol 2007;127:2207–15.

[12] Maddison B, Namazi MR, Samuel LS, Sanchez J, Pichardo R, Stocks J, et al. Unexpected diminished innervation of epidermis and dermoepidermal junction in lichen amyloidosis. Br J Dermatol 2008;159:403–6.

[13] Bando T, Morikawa Y, Komori T, Senba E. Complete overlap of interleukin 31 receptor A and oncostatin M receptor beta in the adult dorsal root ganglia with distinct developmental expression pattern. Neuroscience 2006;142:1263–71.

Ken Arita[a,*]
Riichiro Abe[a]
Keiko Baba[a]
John A. McGrath[b]
Masashi Akiyama[a]
Hiroshi Shimizu[a]

[a]*Department of Dermatology, Hokkaido University Graduate School of Medicine, North 15 West 7, Kita-ku, Sapporo 060-8638, Japan*
[b]*Genetic Skin Disease Group, St. John's Institute of Dermatology, Division of Genetics and Molecular Medicine, King's College London (Guy's Campus), London, UK*

*Corresponding author. Tel.: +81 11 706 7387; fax: +81 11 706 7820
E-mail address: ariken@med.hokudai.ac.jp (K. Arita)

9 January 2009

Immunological Reconstitution after Autologous Hematopoietic Stem Cell Transplantation in Patients with Systemic Sclerosis: Relationship Between Clinical Benefits and Intensity of Immunosuppression

TOSHIYUKI BOHGAKI, TATSUYA ATSUMI, MIYUKI BOHGAKI, AKIRA FURUSAKI, MAKOTO KONDO, KAZUKO C. SATO-MATSUMURA, RIICHIRO ABE, HIROSHI KATAOKA, TETSUYA HORITA, SHINSUKE YASUDA, YOSHIHARU AMASAKI, MITSUFUMI NISHIO, KEN-ICHI SAWADA, HIROSHI SHIMIZU, and TAKAO KOIKE

ABSTRACT. **Objective.** To analyze the relationship between clinical benefits and immunological changes in patients with systemic sclerosis (SSc) treated with autologous hematopoietic stem cell transplantation (HSCT).

Methods. Ten patients with SSc were treated with high-dose cyclophosphamide followed by highly purified CD34+ cells (n = 5) or unpurified grafts (n = 5). Two groups of patients were retrospectively constituted based on their clinical response (good responders, n = 7; and poor responders, n = 3). As well as clinical findings, immunological reconstitution through autologous HSCT was assessed by fluorescence-activated cell sorter analysis, quantification of signal joint T cell receptor rearrangement excision circles (sjTREC), reflecting the thymic function, and *foxp3*, a key gene of regulatory T cells, mRNA levels.

Results. Patients' clinical and immunological findings were similar between good and poor responders, or CD34-purified and unpurified groups at inclusion. The sjTREC values were significantly suppressed at 3 months after autologous HSCT in good responders compared with poor responders (p = 0.0152). Reconstitution of CD4+CD45RO- naive T cells was delayed in good responders compared with poor responders. The phenotype of other lymphocytes, cytokine production in T cells, and *foxp3* gene expression levels after autologous HSCT did not correlate with clinical response in good or poor responders. Clinical and immunological findings after autologous HSCT were similar between CD34-purified and unpurified groups.

Conclusion. Our results suggest that immunosuppression intensity, sufficient to induce transient suppression of thymic function, is attributable to the feasible clinical response in patients with SSc treated with autologous HSCT. Appropriate monitoring of sjTREC values may predict clinical benefits in transplanted SSc patients after autologous HSCT. (First Release May 15 2009; J Rheumatol 2009;36:1240–8; doi:10.3899/jrheum.081025)

Key Indexing Terms:
SYSTEMIC SCLEROSIS   HEMATOPOIETIC STEM CELL TRANSPLANTATION
              IMMUNOLOGICAL RECONSTITUTION

From the Department of Medicine II and the Department of Dermatology, Hokkaido University Graduate School of Medicine, Sapporo; and Third Department of Internal Medicine, Akita University School of Medicine, Akita, Japan.

Supported by a grant from the Japanese Ministry of Health, Labor and Welfare.

T. Bohgaki, MD, PhD; T. Atsumi, MD, PhD; M. Bohgaki, MD, PhD; A. Furusaki, MD, PhD; M. Kondo, MD, PhD, Department of Medicine II; K.C. Sato-Matsumura, MD, PhD; R. Abe, MD, PhD, Department of Dermatology; H. Kataoka, MD, PhD; T. Horita, MD, PhD; S. Yasuda, MD, PhD; Y. Amasaki, MD, PhD; M. Nishio, MD, PhD, Department of Medicine II, Hokkaido University Graduate School of Medicine; K. Sawada, MD, PhD, Third Department of Internal Medicine, Akita University School of Medicine; H. Shimizu, MD, PhD, Department of Dermatology; T. Koike, MD, PhD, Department of Medicine II, Hokkaido University School of Medicine.

Address reprint requests to Dr. T. Atsumi, Department of Medicine II, Hokkaido University Graduate School of Medicine, N15, W7, Kita-ku, Sapporo 060-8638, Japan. E-mail: at3tat@med.hokudai.ac.jp

Accepted for publication January 8, 2009.

Systemic sclerosis (SSc) is an autoimmune disease characterized by the presence of skin sclerosis, organ fibrosis, and autoantibodies[1]. Despite extensive research on autoimmunology and endotheliology, its pathophysiology has been far from conclusive[2,3]. The skin and organ manifestations of SSc are, in general, slowly progressive and chronically disabling. In some patients, however, they can be rapidly progressive and fatal due to organ involvements such as interstitial pneumonia, arrhythmia, and renal failure. Severe organ involvement frequently occurs within the first 3 years of disease[1]. These clinical features affect daily living activity and life expectancy in patients with SSc.

Autologous hematopoietic stem cell transplantation (HSCT) has been indicated for patients with autoimmune diseases, resulting in great success particularly in patients with SSc[4-10]. Autologous HSCT is one of the treatments in

patients suffering from hematological malignant diseases. For the practice of autologous HSCT against those malignant diseases, graft manipulation using antibody specific for CD34, a marker of human hematopoietic stem cells, is usually essential to deplete malignant cells from the graft. On the other hand, patients treated with CD34+-selected autologous HSCT (CD34-HSCT) may have infectious complications during hematological recovery more frequently than patients treated with unselected autologous HSCT (unselected-HSCT)[11]. The graft manipulation was performed in many patients with severe autoimmune diseases treated by autologous HSCT in consideration of depleting autoreactive lymphocytes and inducing profound clinical remission. Meanwhile, it has been debated whether CD34+ cell selection in the graft is necessary or not[9,12].

The difference in conditioning regimens is not related to the clinical benefits, and about one-third of transplanted patients do not benefit from these intensive immunosuppressive treatment[9,13]. Clinical response may depend on profound qualitative immunological changes obtained by autologous HSCT in patients with systemic lupus erythematosus or multiple sclerosis[14,15]. Little is known as to why and how patients with SSc have clinical benefits of autologous HSCT. The aim of our study was to elucidate the relationship between clinical effect and alteration of immunological profiles in patients with SSc treated with autologous HSCT.

MATERIALS AND METHODS

Patients. Our study was approved by the ethical committee of Hokkaido University and written informed consent was obtained from all participants. Thirty-one patients with SSc, all of whom met the American College of Rheumatology preliminary criteria[16], were screened for our study. All patients developing SSc within the last 3 years onset fulfilled at least 1 of the following: early rapidly progressive diffuse skin sclerosis despite continuing treatment, refractory skin ulcers, interstitial lung disease confirmed by lung computed tomography (CT), reversible cardiac involvement such as arrhythmia and cardiomegaly, renal involvement with hypertension, persistent urinalysis abnormalities, and microangiopathic hemolytic anemia. Patients were excluded from the study when they were over 60 years old, or had uncontrolled arrhythmia, left ventricular ejection fraction on echocardiography below 45%, carbon dioxide diffusion lung capacity (DLCO) below 45% predicted, serum creatinine above 176.8 μmol/L (2.0 mg/dl) and glomerular filtration rate (GFR) below 40 ml/min/m^2. All enrolled patients were evaluated clinically at the time of diagnosis and on regular visits for followup.

Thirty-five healthy controls were also enrolled in the study.

Transplantation procedure and followup. The mobilization regimen comprised recombinant human granulocyte colony-stimulating factor (rhG-CSF) and intravenous cyclophosphamide (4 g/m^2). In 5 patients treated with CD34-HSCT, enriched CD34+ graft, prepared using CliniMACS® system (Miltenyi Biotec, Germany) was stored in liquid nitrate until use for transplant. Graft manipulation was not performed in the next 5 patients treated with unselected-HSCT.

We treated all SSc patients with intravenous cyclophosphamide (200 mg/kg, divided into 4 days) followed by autologous HSCT. rhG-CSF was administered from the second day of transplantation of frozen-thawed autologous enriched CD34+ grafts or frozen-thawed autologous unselected grafts. T cell depleting antibodies such as antithymocyte globulin, antilym-

phocyte globulin and anti-CD52 antibodies (Campath) were not administered in our patients.

We assessed the improvement of skin sclerosis by the modified Rodnan total thickness skin score (mRTSS). Electrocardiogram and echocardiography were used to evaluate the cardiac function, chest radiograph, chest high resolution CT, and spirometry to evaluate pulmonary function, renogram to evaluate renal function, and serological tests to assess other organ involvement and the presence of autoantibodies.

Lymphocyte phenotyping. Peripheral blood mononuclear cells (PBMC) were prepared from heparinized venous blood by Ficoll-Paque Plus® (Amersham Biosciences Corp., NJ, USA).

We assessed the subpopulation of peripheral lymphocytes by immunofluorescence staining of PBMC with anti-human CD3-Cy-Chrome, CD4-fluorescein isothiocyanate (FITC), CD8-FITC, CD19-FITC, TCRγδ-FITC, CD3-phycoerythrin (PE), CD8-PE, CD45RO-PE, CD25-PE, HLA-DR-PE, and CD69-PE (BD Biosciences Pharmingen, San Diego, CA).

The expression levels of interferon (IFN)-γ and interleukin (IL)-4 were studied in the cytoplasm of peripheral CD4+ or CD8+ T cells. Briefly, we stimulated PBMC with phorbol myristate acetate (50 ng/ml) and ionomycin (250 ng/ml) for 6 h in RPMI 1640 containing 10% heat-inactivated fetal bovine serum and monensin (2 μM) at 37°C in 5% carbon dioxide. We evaluated the IFN-γ or IL-4 expression on T cells by staining with anti-CD3-Cy-Chrome, anti-CD8-FITC and -PE, anti-IFN-γ-FITC, and anti-IL-4-PE using Cytofix/Cytoperm Plus® (BD Biosciences Pharmingen) according to the manufacturer's instructions. Immunostained cells were analyzed using a FACSCalibur™ flow cytometer (Becton Dickinson Immunocytometry Systems, San Jose, CA).

Quantification of thymic signal joint T cell receptor rearrangement excision circles (sjTREC). Thymic sjTREC on genomic DNA from PBMC was quantified by real-time quantitative polymerase chain reaction (PCR) (ABI PRISM® 7000; Applied Biosystems, Foster City, CA) according to the method of Douek, *et al*[17]. The sjTREC values were corrected by the percentage of CD3+ cells in the sample and were then expressed as numbers of sjTREC/μg of CD3+ cells DNA according to the method of Farge, *et al*[18]. Values were measured before autologous HSCT, then at 3, 6, and 12 months after autologous HSCT.

Quantification of foxp3 *gene expression levels.* Total RNA were isolated from PBMC using TRIzol® reagent (Invitrogen, Carlsbad, CA) according to the manufacturer's instructions. Total RNA (1 μg) was reverse transcribed by ReverTraAce (Toyobo, Osaka, Japan), in the presence of oligo(dT)12-18 primers (Invitrogen) according to the manufacturer's instructions. We performed real-time PCR using the ABI PRISM® 7000 Sequence Detection System and specific primers for *foxp3* and *gapdh* from TaqMan® Gene Expression Assays (Applied Biosystems).

Statistical analysis. We used the Mann-Whitney U-test to analyze the difference among each value otherwise indicated. The changes in mRTSS and phenotype of lymphocytes after the autologous HSCT were compared with values at inclusion using the Wilcoxon signed rank test. Female-male ratio in each group was assessed using Fisher's exact probability test. The sjTREC values in healthy individuals were assessed using the Spearman's correlation test. Calculations were performed using the statistical software package JMP version 5.0 (SAS Institute Inc., Cary, NC). P values less than 0.05 were considered significant.

RESULTS

Between November 2000 and July 2006, 11 consecutive patients meeting the criteria in our study were enrolled and 10 patients were transplanted out of 31 screened patients with SSc for autologous HSCT treatment. One patient was not transplanted because of her mobilization failure. First 5 patients were treated with CD34-HSCT. Subsequent 5 patients were treated with unselected-HSCT. The character-

istics of patients treated with autologous HSCT are shown in Table 1. Mean age at inclusion, mean mRTSS before mobilization and mean durations from SSc onset to the treatment were similar between patients treated with CD34-HSCT and unselected-HSCT. Several treatments such as D-penicillamine, prostaglandin derivatives, and corticosteroids were not feasible for our patients. All patients were followed up until July 2007 (40.7 ± 25.6 mos).

Mean number of infused CD34+ cells was not different between CD34-HSCT and unselected-HSCT groups. Mean time needed to achieve a neutrophil count greater than $0.5 \times 10^9/l$ and a platelet count greater than $50 \times 10^9/l$ were not different between 2 groups. Cytomegalovirus antigenemia were shown in 3 patients out of all transplanted patients. Patient 2 had hemophagocytic syndrome on day 6. Patient 3 had adenoviral hemorrhagic cystitis on day 14 and engraftment syndrome on day 15. Patient 7 had engraftment syndrome on day 12. Hemophagocytic syndrome and engraftment syndrome responded to corticosteroid administration. Hemorrhagic cystitis was refractory to acyclovir, vidarabine, ganciclovir, or ribavirin. Patient 3 had the second autologous HSCT using unselected grafts at 3 months after first autologous HSCT using selected CD34+ cells due to recurrent infectious diseases.

Four out of 5 transplanted patients have more than a 25% fall in the skin score compared with baseline values in both groups (Figure 1). Dermal thickness assessed by skin biopsy was also improved in these patients with clinical benefits (data not shown). Additional unselected-HSCT at 3 months after CD34-HSCT did not affect Patient 3's skin manifestation. Cardiac and pulmonary functions were not altered significantly through the treatment in all patients (data not shown). Their serum level of γ-globulin almost remained normal range through autologous HSCT (data not shown). Their serum level of anti-Scl70 antibodies reduced except Patient 2 treated with CD34-HSCT (data not shown). Transplantation related complications during hospitalization are shown in Table 1. There was no significant difference in the incidence of adverse events between both groups and no transplantation related mortality.

We compared immunological reconstitution profile over time between good and poor response groups, and between CD34-HSCT and unselected-HSCT groups. First, we analyzed immunological reconstitution between good and poor response groups. Clinical response to therapy was categorized into major, partial, or no response, or disease progression or relapse according to the method of Farge, et al[13]. According to the observed clinical response compared to these criteria, 2 groups of patients were retrospectively constituted: good response group, consisting of 7 patients with sustained major or partial response, and poor response group, consisting of 3 patients (Patient 5, 6, and 7) with no

Table 1. Patients' profile at study inclusion and clinical findings at autologous hematopoietic stem cell transplantation (HSCT).

| | Patients Treated with CD34-HSCT | | | | | Patients treated with Unselected-HSCT | | | | | Mean ± SD | | |
	1	2	3	4	5	6	7	8	9	10	CD34	Untreated	p
Age, yrs	57	19	54	48	52	43	19	42	30	28	46.0 ± 15.4	32.4 ± 10.1	0.094
Sex, female:male	M	F	F	F	M	M	F	F	F	F	3:2	4:1	1.000
mRTSS, 0–51	38	28	25	15	32	32	17	26	23	20	27.6 ± 8.6	23.6 ± 5.8	0.402
Disease duration, mo	21	31	21	12	36	16	24	18	8	12	24.2 ± 9.4	15.6 ± 6.1	0.141
Interstitial pneumonia	—	—	+	—	+	—	+	—	—	—	—	—	—
GFR, ml/min	76.53	121.43	101.43	114.39	99.32	139.29	120.3	101.8	82.62	103.42	102.6 ± 17.2	109.5 ± 21.3	0.465
DLCO %	83	66.8	52.2	90.9	83.8	92.5	54.7	113.4	48	94.4	75.3 ± 15.7	80.6 ± 28.0	0.465
γ-globulin, %	19.5	24.7	24.1	16.8	12.5	20.5	19.8	—	16.8	16.7	19.5 ± 5.1	18.5 ± 2.0	0.712
Anti-Scl 70, index	< 5	92.3	204.6	8.7	158.6	16.1	128.2	< 5	< 5	202	92.8 ± 90.2	69.3 ± 91.5	0.597
Prior therapies	PG	PG, D, PSL	PG, PSL	PG, PSL	D, PSL	PG	PG	D, PSL	D, PSL	PG	—	—	—
Mobilization	G	G + CYC	G + CYC	G + CYC	G + CYC	G + CYC	G + CYC	G + CYC	G + CYC	G + CYC	—	—	—
Conditioning	CYC	CYC	CYC	CYC	CYC	CYC	CYC	CYC	CYC	CYC	—	—	—
Infused CD34+ cells, × 10^6/kg	2.96	5.21	2.75	3.14	12.7	3.95	2.77	4.28	14.9	2.81	5.4 ± 4.2	5.7 ± 5.2	0.917
Purity, %	96	95	90	93.53	96.59	—	—	—	—	—	94.2 ± 2.6	—	—
Neutrophils > 0.5 × 10^9/l (day)	11	9	11	9	9	8	11	10	10	10	9.8 ± 1.1	9.8 ± 1.1	0.914
Platelets > 50 × 10^9/l (day)	15	21	16	8	11	0	8	11	11	12	14.2 ± 5.0	8.4 ± 4.9	0.138
Transplant related complications	CMV	CMV, HPS	CMV, HC, ES	—	—	—	ES	—	—	—	—	—	—

mRTSS: modified Rodnan total thickness skin score; PG: prostaglandin derivatives; D: d-penicillamine; PSL: prednisolone; G: granulocyte-colony-stimulating factor; CYC: cyclophosphamide; CMV: cytomegalovirus antigenemia; HPS: hemophagocytic syndrome; HC: hemorrhagic cystitis; ES: engraftment syndrome; GFR: glomerular filtration rate; DLCO: diffusion capacity for carbon monoxide.
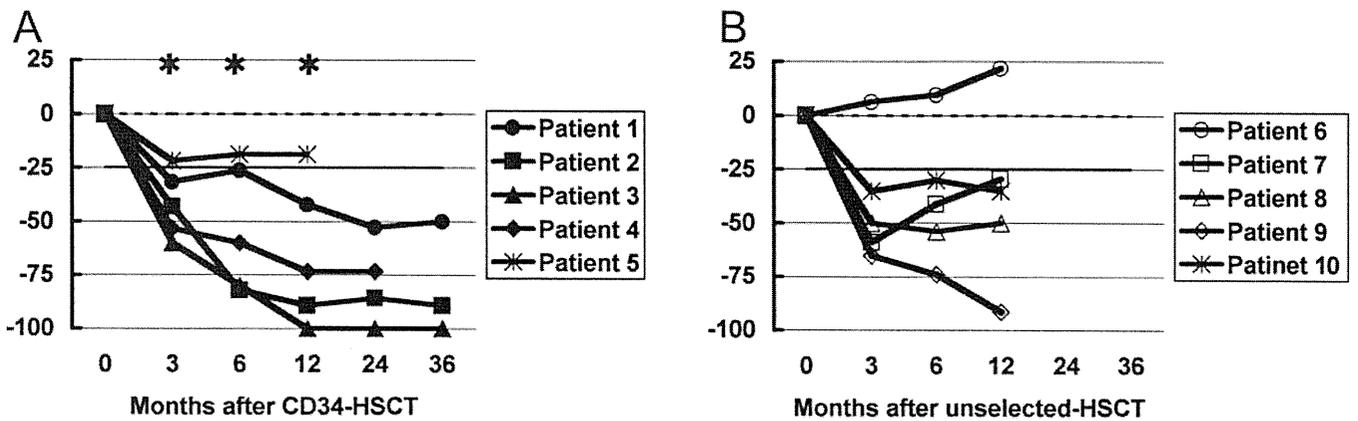
—279—

Figure 1. Evaluation of modified Rodnan total thickness skin score (mRTSS) in patients with systemic sclerosis. A. Changes of mRTSS in patients treated with CD34-HSCT. B. Changes of mRTSS in patients treated with unselected-HSCT. Proportional change from baseline measurement was calculated for each patient at each available timepoint. * p < 0.05.

response or with relapse of disease (Table 2). Our patients were evaluated by functional evaluation (performance status and/or health assessment questionnaire) and mRTSS with skin improvement assessed by skin biopsy. Each organ function was not altered significantly through the treatment in all patients. Mean age at inclusion, mean mRTSS before mobilization, and mean durations from onset scleroderma to treatment were similar between both groups. At inclusion, the ratio of CD4/CD8, the percentage of CD4+CD45RO+, CD4+CD45RO-, CD19+, CD4+CD25+, CD56+, CD3+TCRγδ+, IFN-γ- and IL-4-producing CD4+ and CD8+ cells were in the normal range for all patients and were not different between good and poor response groups (Table 3). After autologous HSCT, shortened CD4/CD8 ratio was sustained due to delayed CD4+ cell recovery and prompt CD8+ cell recovery in both groups. CD4+CD45RO-naive T cells remained low at 6 months after autologous HSCT in good response group, and CD4+CD45RO- cells reconstituted faster in poor response group (p < 0.05). CD19+ and CD56+ cells returned into the normal range at 3 months in both groups. The kinetics of other cells through autologous HSCT was not statistically different between good and poor response group in the

study. To evaluate the T cell response against mitogen stimulation after autologous HSCT, mean fluorescence intensity of CD69 on CD3+ cells was investigated. CD69 expression levels on CD3+CD8+ and CD3+CD8- cells against mitogen were not different between healthy controls and patients with SSc before autologous HSCT, and its kinetics through autologous HSCT were similar in both groups (Table 3). Cytokine production in CD3+CD8- and CD3+CD8+ T cells was assessed by intracellular staining of IFN-γ and IL-4. Levels of cytokine production in CD3+CD8- and CD3+CD8+ cells were not different between both groups. IFN-γ producing CD8+ T cells increased after autologous HSCT in both groups (Table 3).

Thymic output assessed by sjTREC was analyzed to evaluate the mechanism of peripheral CD4+CD45RO- and CD4+CD25+ proliferation. In healthy controls, the sjTREC values negatively correlated with their age (Figure 2A, p < 0.0001, $r^2 = 0.44$). Nine out of 10 transplanted patients could be analyzed in the study. Their sjTREC values also negatively correlated with their age at inclusion of autologous HSCT (Figure 2B, p = 0.002, $r^2 = 0.80$). The sjTREC values were not significantly different between patients with SSc before autologous HSCT and age- and sex-matched

Table 2. Patients' profile between good and poor response groups at autologous HSCT.

	Good Response Group (n = 7)	Poor Response Group (n = 3)	p
Graft condition (CD34-HSCT: unselected)	4:3	1:2	1.000
Age, yrs	39.7 ± 14.4	38.0 + 17.1	0.819
Sex female: male	6:1	1:2	1.000
mRTSS (0–51)	25.0 ± 7.16	27.0 ± 8.66	0.568
Disease duration, mo	17.6 ± 7.72	25.3 ± 10.1	0.207
Infused CD34+ cells (× 10^6/kg)	5.15 ± 4.39	6.47 ± 5.42	0.909
Neutrophils > 0.5 × 10^9/l (day)	10.0 ± 0.82	9.33 ± 1.53	0.407
Platelets > 50 × 10^9/l (day)	13.4 ± 4.28	6.33 ± 5.69	0.064

mRTSS: modified Rodnan total thickness skin score.

—280—

Table 3. Phenotype analysis of lymphocyte population through autologous HSCT between patients with good and poor clinical response. Value are mean ± SD.

	Normal Range 95% CI	At Inclusion Good	Poor	3 mo After HSCT Good	Poor	6 mo After HSCT Good	Poor	12 mo After HSCT Good	Poor
CD3+, CD4+	57.57–68.89	48.16 ± 18.77	52.34 ± 6.56	20.84 ± 9.75*	34.42 ± 7.66	23.18 ± 15.00*	45.23 ± 10.74	27.65 ± 15.61***	43.07 ± 9.72
CD3+, CD8+	26.47–37.68	25.91 ± 9.32	33.92 ± 13.66	48.07 ± 21.57	49.64 ± 11.44	35.78 ± 15.44	49.69 ± 13.09	44.97 ± 13.94	47.56 ± 10.43
CD4/CD8	0.61–2.96 (ratio)	2.11 ± 1.31	1.74 ± 0.72	0.43 ± 0.13*	0.71 ± 0.15	0.66 ± 0.35*	1.01 ± 0.56	0.61 ± 0.28	0.96 ± 0.39
CD3+, TCRγδ+	0.74–9.48	3.03 ± 3.05	2.03 ± 1.19	5.11 ± 4.49	2.34 ± 0.84	2.75 ± 1.48	3.02 ± 1.86	4.18 ± 2.72	2.71 ± 1.80
CD4+, CD45RO–	5.23–42.08	28.51 ± 10.29	31.36 ± 8.40	3.43 ± 2.49*	7.89 ± 5.21	4.66 ± 2.93*	10.01 ± 8.46	7.12 ± 5.18	12.55 ± 10.78
CD4+, CD45RO+	9.00–27.97	17.08 ± 5.53	15.35 ± 3.87	15.48 ± 6.23	19.34 ± 5.87	13.68 ± 7.31	16.42 ± 4.85	14.32 ± 4.08	13.89 ± 4.10
CD4+, HLA-DR+	0.92–3.38	2.38 ± 0.86	3.95 ± 2.10	8.51 ± 4.99	12.58 ± 3.23	5.77 ± 4.58	7.12 ± 0.50	5.36 ± 4.16	5.20 ± 2.46
CD4+, CD25+	1.35–5.46	4.12 ± 3.36	5.45 ± 2.79	3.42 ± 2.21	6.12 ± 5.51	3.43 ± 2.67	7.54 ± 3.36	3.55 ± 2.28	4.62 ± 3.92
foxp3 mRNA	32.01–393.07 (copies/GAPDH 1 k copies)	563.39 ± 704.09	259.60 ± 247.27	182.74 ± 150.35	99.31 ± 29.61	201.77 ± 114.85	212.28 ± 121.62	214.00 ± 109.77	166.29 ± 133
CD3+, CD8–, IFNγ+	0.67 ± 17.49	6.05 ± 6.55	2.73 ± 0.60	12.16 ± 10.07	7.06 ± 5.20	8.21 ± 5.36	11.47 ± 8.02	9.29 ± 4.17	4.23 ± 3.66
CD3+, CD8–, IL4+	0.02–2.47	1.09 ± 0.55	1.39 ± 1.30	3.74 ± 2.63	2.50 ± 1.04	2.40 ± 2.13	4.96 ± 6.27	1.57 ± 1.24	1.20 ± 0.58
Th1/Th2	3.79–125.60 (ratio)	17.38 ± 21.04	4.98 ± 3.77	32.47 ± 52.40	107.75 ± 154.29	32.09 ± 45.55	67.05 ± 59.15	24.82 ± 23.42	23.75 ± 36.56
CD3+, CD8+, IFNγ+	0.66–41.60	5.73 ± 6.15	5.25 ± 3.11	29.83 ± 21.39*	19.80 ± 11.29	17.43 ± 13.55	25.93 ± 13.92	27.71 ± 19.13	3.29 ± 4.95
CD3+, CD8+, IL4+	0.00–1.40	0.19 ± 0.17	0.25 ± 0.38	0.86 ± 0.79	0.54 ± 0.38	1.01 ± 1.24	0.68 ± 0.68	0.72 ± 0.45	0.16 ± 0.15
Tc1/Tc2	7.83–185.08 (ratio)	89.68 ± 98.17	56.15 ± 71.29	154.35 ± 217.62	1492.65 ± 2280.82	88.36 ± 78.79	1460.06 ± 1262.52	80.27 ± 76.12	41.91 ± 71.92
CD3+, CD8–, CD69+	82.91–201.89 (MFI)	177.55 ± 90.61	121.10 ± 84.95	58.25 ± 41.65	28.34 ± 12.87	63.06 ± 37.00	67.76 ± 40.69	89.54 ± 42.85	38.52 ± 33.83
CD3+, CD8+, CD69+	54.27–119.07 (MFI)	106.82 ± 35.27	96.05 ± 64.04	30.92 ± 20.39	24.94 ± 12.97	31.00 ± 19.98	53.89 ± 30.39	61.82 ± 19.69	30.83 ± 19.29
CD19+	5.00–32.98	16.16 ± 7.54	12.69 ± 9.40	21.91 ± 22.58	14.40 ± 7.64	27.01 ± 22.93	9.50 ± 5.73	18.60 ± 10.83	11.13 ± 3.99
CD56+	8.94–22.94	13.17 ± 11.67	11.83 ± 7.68	14.11 ± 6.97	9.93 ± 4.49	8.99 ± 2.96	19.83 ± 11.87	12.05 ± 7.58	14.12 ± 7.61

* The value from the baseline measurement was calculated for each value at each timepoint. p < 0.05. MFI: mean fluorescence intensity.

healthy controls (p = 0.8253). The sjTREC values were significantly suppressed at 3 months after autologous HSCT in the good response group compared with poor responders (Figure 2C, p = 0.0152), although the values were not different at inclusion, 6 and 12 months after autologous HSCT between both groups.

Foxp3 is a key regulatory gene for the development of regulatory T cells[19]. *Foxp3* gene expressions in PBMC were analyzed to assess the relationship between the recovery of CD4+CD25+ cells including regulatory T cells and clinical benefits in transplanted SSc patients. *Foxp3* gene expressions in PBMC were within the normal range through autologous HSCT and were not different in the 2 groups (Table 3).

Next, immunological reconstitution was analyzed between CD34-HSCT and unselected-HSCT groups to assess how graft manipulation affected immune system and clinical response. At inclusion, the ratio of CD4/CD8, the percentage of CD4+CD45RO–, CD4+CD45RO+, CD19+, CD4+CD25+, CD56+, CD3+TCRγδ+, IFN-γ, and IL-4 producing CD4+ and CD8+ cells were in the normal range for all patients and did not differ between CD34-HSCT and unselected-HSCT. After autologous HSCT, CD4/CD8 ratio remained low in both groups. In CD4+ subsets, CD4+CD45RO–, CD4+HLA-DR+, and CD4+CD25+ cells

increased rapidly in unselected-HSCT compared with CD34-HSCT at 12 months (p < 0.05, Table 4). CD19+ and CD56+ cells returned into the normal range at 3 months in both groups. CD69 expression levels on CD3+CD8+ and CD3+CD8– cells against mitogen were not different between healthy controls and patients with SSc before autologous HSCT, and its kinetics through autologous HSCT were similar in both groups (Table 4). Levels of cytokine production in CD3+CD8– and CD3+CD8+ cells were not different between both groups. IFN-γ-producing CD3+CD8+ T cells increased after autologous HSCT in both groups (Table 4).

Cytokine production in CD8– and CD8+ T cells was assessed by intracellular IFN-γ and IL-4. Cytokine production in CD8– cells was not different between both groups. IFN-γ- and IL-4-producing CD8+ T cells increased after autologous HSCT in both groups (Table 4).

The sjTREC values recovered to the levels at inclusion between 6 to 12 months after CD34-HSCT or unselected-HSCT. There was no statistical significance through their clinical course in both groups (Figure 2D).

Foxp3 gene expressions in PBMC were within the normal range through autologous HSCT and not different in the 2 groups (Table 4).
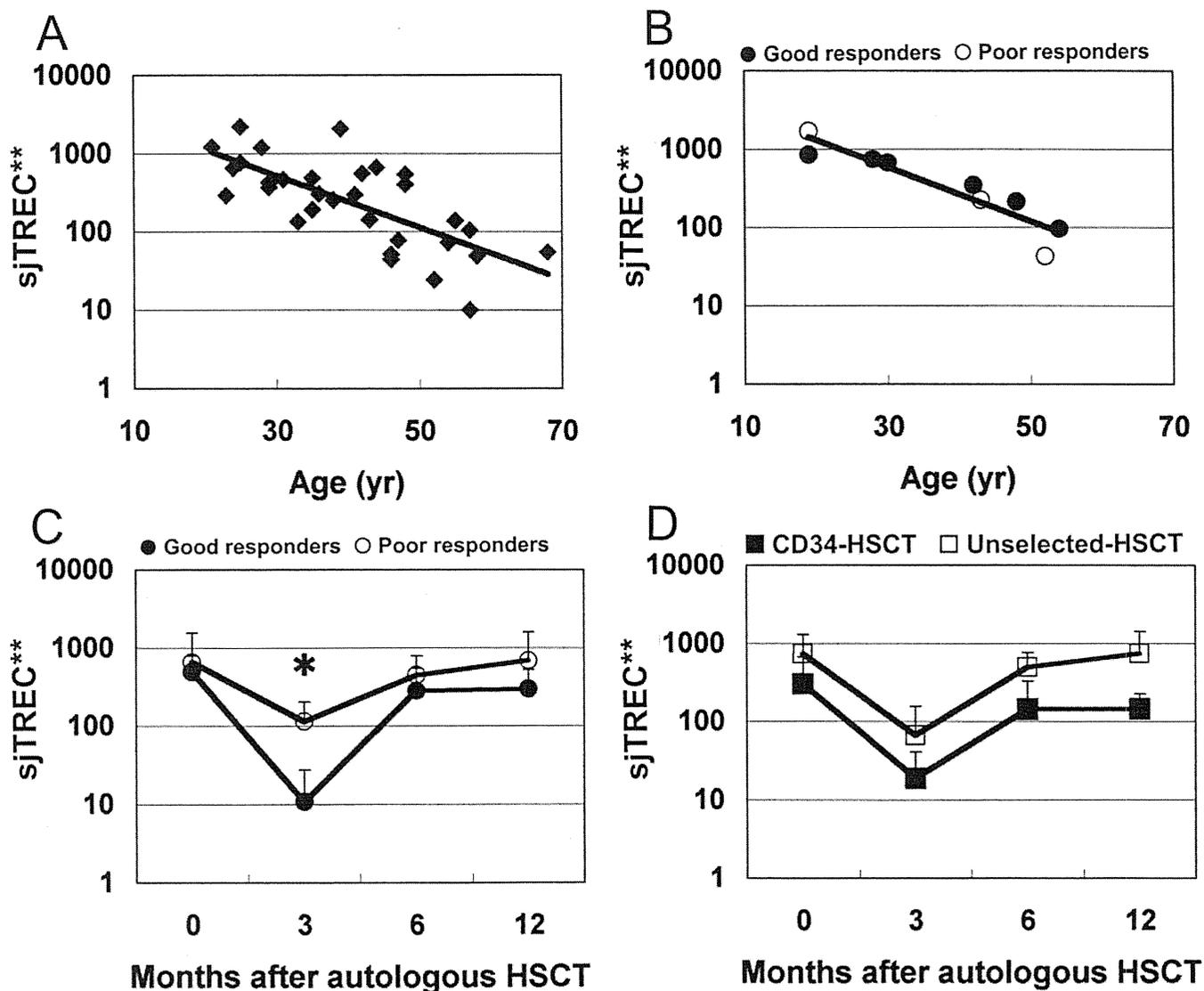
Figure 2. sjTREC values in CD3+ cells in healthy individuals and its kinetics through autologous HSCT. A. Relation between age and numbers of sjTRECs in healthy controls. B. Relation between age and numbers of sjTREC in SSc patients treated with autologous HSCT. C. sjTREC between good and poor response groups. D. sjTREC between patients treated with CD34-HSCT and unselected-HSCT. Logarithmic scales were used for y-axes to compress the figure. * p = 0.0152. **copies/μg in CD3+ cells DNA.

DISCUSSION

We described the efficacy and the safety in patients with SSc treated with autologous HSCT. More than a 25% decrease in the skin score, which correlates with patient's survival[20], was achieved in 8 out of 10 transplanted SSc patients. Skin improvement was not significantly different between CD34-HSCT and unselected-HSCT groups. In addition, additional unselected-HSCT did not lead to recurrence or adverse effect on skin manifestation in Patient 3. These results suggest that graft condition did not affect the clinical outcome on skin involvement up to 12 months after autologous HSCT in our series.

Few data on thymic function and lymphocyte phenotypes after autologous HSCT have been reported in transplanted SSc patients[13,18,21]. The TREC values might be related to clinical response in our transplanted patients. In the last decade, basic and clinical scientists have focused a role of sjTREC as a marker of human thymic function[22]. Values of sjTREC can also reflect the pathophysiology in patients with autoimmune diseases. The sjTREC values may be affected by disease activity in patients with systemic lupus erythematosus[23]. Age-inappropriate T cell senescence confirmed by decreased frequency of sjTREC may also contribute to the development of juvenile idiopathic arthritis[24]. There was no evidence to prove an age-inappropriate T cell senescence and a correlation between the sjTREC values

Table 4. Phenotype analysis of lymphocyte population through autologous HSCT between patients with CD34-HSCT and unselected-HSCT. Values are mean ± SD.

	Normal Range 95% CI	At Inclusion CD34–HSCT	un-HSCT	3 mo After HSCT CD34-HSCT	un-HSCT	6 mo After HSCT CD34-HSCT	un-HSCT	12 mo After HSCT CD34-HSCT	un-HSCT
CD3+, CD4+	57.57–68.89	37.84 ± 11.45	60.99 ± 9.66	17.85 ± 9.95	31.98 ± 6.69*	20.30 ± 14.73	43.31 ± 9.75	24.13 ± 14.36*	43.62 ± 8.46
CD3+, CD8+	26.47–37.68	22.20 ± 6.45	34.42 ± 11.06	36.07 ± 18.09	61.02 ± 6.96	33.69 ± 15.89	48.83 ± 11.58	42.02 ± 14.06	50.60 ± 9.08
CD4/CD8	0.61–2.96 (ratio)	1.87 ± 0.87	2.13 ± 1.45	0.49 ± 0.22*	0.54 ± 0.18*	0.62 ± 0.36*	0.97 ± 0.48	0.58 ± 0.28*	0.91 ± 0.35
CD3+, TCRγδ+	0.74–9.48	3.66 ± 3.44	1.80 ± 1.09	4.31 ± 5.13	4.24 ± 2.90	2.54 ± 1.62	3.21 ± 1.48	4.03 ± 2.78	2.85 ± 1.52
CD4+, CD45RO–	5.23–42.08	29.10 ± 7.34	29.63 ± 12.01	4.58 ± 5.44*	4.95 ± 1.91*	4.94 ± 3.36*	8.33 ± 7.59	4.29 ± 2.23*	14.73 ± 7.39
CD4+, CD45RO+	9.00–27.97	15.56 ± 4.16	17.57 ± 5.93	13.79 ± 6.90	19.48 ± 3.92	14.20 ± 7.61	15.09 ± 5.65	13.02 ± 3.83	16.32 ± 2.91
CD4+, HLA-DR+	0.92–3.38	2.90 ± 1.36	2.80 ± 1.66	7.61 ± 5.72	11.85 ± 2.72	4.36 ± 2.32	8.54 ± 4.03	2.92 ± 0.56	8.29 ± 3.34
CD4+, CD25+	1.35–5.46	2.70 ± 1.67	6.33 ± 3.28	2.30 ± 1.10	5.94 ± 4.07	3.33 ± 3.20	6.64 ± 2.98	2.02 ± 0.95	6.27 ± 2.24
foxp3 mRNA	32.01–393.07 (copies/GAPDH 1k copies)	524.44 ± 880.90	420.07 ± 199.61	110.72 ± 100.54	204.72 ± 149.57	129.22 ± 101.19	280.62 ± 51.70	123.34 ± 60.37	291.54 ± 87.8
CD3+, CD8–, IFNγ+	0.67–17.49	6.65 ± 8.28	3.58 ± 1.62	13.59 ± 10.75	7.95 ± 6.99	9.60 ± 4.19	9.27 ± 8.38	5.64 ± 3.27	17.44 ± 10.45
CD3+, CD8–, IL4+	0.02–2.47	0.85 ± 0.59	1.46 ± 0.89	4.51 ± 2.41	2.38 ± 1.75	2.98 ± 1.95	3.74 ± 5.68	1.97 ± 0.90	0.61 ± 0.31
Th1/Th2	3.79–125.60 (ratio)	20.41 ± 26.40	7.51 ± 4.67	13.88 ± 15.28	96.22 ± 120.52	31.49 ± 37.45	68.90 ± 75.09	13.81 ± 23.54	37.78 ± 25.33
CD3+, CD8+, IFNγ+	0.66–41.60	8.31 ± 6.99	3.38 ± 1.47	27.35 ± 22.64	25.80 ± 17.33	30.29 ± 10.03	10.94 ± 8.31	24.77 ± 25.94	12.34 ± 10.07
CD3+, CD8+, IL4+	0.00–1.40	0.23 ± 0.21	0.20 ± 0.28	1.11 ± 0.83	0.46 ± 0.40	1.26 ± 1.27	0.51 ± 0.65	0.81 ± 0.47	0.22 ± 0.17
Tc1/Tc2	7.83–185.08 (ratio)	49.51 ± 62.39	101.70 ± 103.52	127.14 ± 120.21	984.54 ± 1771.58	550.91 ± 974.27	654.58 ± 1136.02	60.02 ± 89.13	76.82 ± 57.32
CD3+, CD8–, CD69+	82.91–201.89 (MFI)	172.45 ± 122.20	147.75 ± 62.66	59.53 ± 53.14	39.28 ± 18.77	68.95 ± 37.16	57.96 ± 39.23	84.12 ± 47.34	47.57 ± 39.01
CD3+, CD8+, CD69+	54.27–119.07 (MFI)	82.70 ± 45.77	119.66 ± 36.51	18.72 ± 5.52	37.09 ± 20.28	33.35 ± 25.06	49.98 ± 26.42	50.73 ± 14.13	49.30 ± 40.58
CD19+	5.00–32.98	18.20 ± 8.43	12.04 ± 6.42	21.84 ± 28.33	17.47 ± 3.07	24.44 ± 24.80	14.05 ± 4.86	18.12 ± 10.94	13.93 ± 5.86
CD56+	8.94–22.94	13.42 ± 13.69	12.12 ± 6.82	12.67 ± 6.43	13.05 ± 7.12	13.79 ± 11.12	11.11 ± 4.10	14.65 ± 7.56	9.74 ± 5.19

* The value from the baseline measurement was calculated for each value at each timepoint. p < 0.05. MFI: mean fluorescence intensity.

and disease condition in our patients with SSc. Thymic function assessed by sjTREC values is significantly suppressed at engraftment, recovers within 3 months after autologous HSCT, and is age-dependent in adults[17,25]. In our series, the lower level of sjTREC at 3 months after autologous HSCT was shown in the good response group without dependence on their age and graft condition. Longterm defects of CD3+CD4+ cells, especially CD4+CD-45RO-naïve T cells, after autologous HSCT might also reflect profound suppression of thymopoiesis in the good response group. Thymus-dependent immunological reconstitution leads to the T cell precursor reeducation and renewal of the T cell repertoire, and may induce remission of autoimmunity[26,27]. Our results suggest that transient, profound suppression of thymic function might alter immune condition, leading to clinical response in patients with SSc.

Peripheral immunological reconstitution after autologous CD34-HSCT or unselected-HSCT has been well documented in patients with hematological disorders[28-30]. While CD56+ cells, followed by CD19+ cells, recover promptly after autologous HSCT, CD3+ cells, especially CD4+CD-45RO- cells, remain low after autologous HSCT in CD34-HSCT and unselected-HSCT[29,30]. After the initial 2 months of autologous HSCT, IFN-γ-producing CD8+ or

CD8- T cells remain normal or increased[11,30]. In our series, kinetics of lymphocytes recovery is similar to these previous results. In patients with SSc, peripheral blood T cells show a predominantly type 2 T-helper profile, and can induce fibrosis through the production of cytokines, especially IL-4[2]. Cytokine production in T cells at inclusion was not significantly different between our transplanted patients with SSc and healthy controls. The kinetics of IFN-γ- and IL-4-producing T cells after autologous HSCT was not different between CD34-HSCT and unselected-HSCT, or good and poor response groups. Therefore, the significance of cytokine production in T cells after autologous HSCT was not conclusive. In good response group with sustained major or partial response, phenotype or function of peripheral lymphocytes was not significantly different from that of poor response group through autologous HSCT. These results suggest that changes in peripheral immunity were not correlated with clinical response.

CD4+CD25+FOXP3+ regulatory T cells may play a role in the immunological reconstitution leading to the improvement of autoimmune disease or prevention of graft-versus-host disease after autologous or allogeneic HSCT[31,32]. Although CD4+CD25+ population increased at 12 months after autologous HSCT in unselected-HSCT compared with

that in CD34-HSCT, it is noted that there was no difference between good and poor response groups, and *foxp3* gene expression levels did not correlate with the clinical response or with graft condition. CD4+CD25+ populations include non-regulatory activated T cells as well as regulatory T cells[32]. Increased CD4+CD25+ population might reflect the activation of CD4+ T cells because CD4+HLA-DR+ population also increased at 12 months in unselected-HSCT group. Therefore, the role of CD4+CD25+ regulatory T cells on clinical response was not evident in our study.

Although the importance of graft manipulation in autologous HSCT for autoimmune diseases has been debated, clinical outcome may not necessarily correlate with the autoreactive clone survival after CD34-HSCT[33]. In patients with rheumatoid arthritis, a pilot study showed that clinical response and laboratory findings were also similar between CD34-HSCT and unselected-HSCT[12]. In addition, autoimmunity after autologous HSCT may result from the type of conditioning regimen rather than graft condition (i.e., CD34-HSCT or unselected-HSCT)[34]. Although peripheral immunity after autologous HSCT does not have a decisive impact on disease control in our transplanted SSc patients, further study will reveal the role of peripheral immunity after autologous HSCT. Our results suggest the relationship between clinical benefits and immunosuppression intensity sufficient to suppress thymic output by the treatment.

The results of our study suggest that immunosuppression sufficient to downregulate thymic function, rather than the graft manipulation, can lead to clinical benefits in patients with SSc. Additionally, appropriately monitoring the sjTREC values after autologous HSCT may serve to identify patients who would not achieve clinical remission by autologous HSCT and additional treatment in a more timely way.

ACKNOWLEDGMENT

REFERENCES

1. Charles C, Clements P, Furst DE. Systemic sclerosis: hypothesis-driven treatment strategies. Lancet 2006;367:1683-91.
2. Sakkas LI, Chikanza IC, Platsoucas CD. Mechanisms of Disease: the role of immune cells in the pathogenesis of systemic sclerosis. Nat Clin Pract Rheumatol 2006;2:679-85.
3. Varga J, Abraham D. Systemic sclerosis: a prototypic multisystem fibrotic disorder. J Clin Invest 2007;117:557-67.
4. Alaez C, Loyola M, Murguia A, et al. Hematopoietic stem cell transplantation (HSCT): an approach to autoimmunity. Autoimmun Rev 2006;5:167-79.
5. Sykes M, Nikolic B. Treatment of severe autoimmune disease by stem-cell transplantation. Nature 2005;435:620-7.
6. Passweg J, Tyndall A. Autologous stem cell transplantation in autoimmune diseases. Semin Hematol 2007;44:278-85.
7. Vonk MC, Marjanovic Z, van den Hoogen FH, et al. Long-term follow-up results after autologous haematopoietic stem cell transplantation for severe systemic sclerosis. Ann Rheum Dis 2008;67:98-104.
8. Nash RA, McSweeney PA, Crofford LJ, et al. High-dose immunosuppressive therapy and autologous hematopoietic cell transplantation for severe systemic sclerosis: long-term follow-up of the US multicenter pilot study. Blood 2007;110:1388-96.
9. Farge D, Passweg J, van Laar JM, et al. Autologous stem cell transplantation in the treatment of systemic sclerosis: report from the EBMT/EULAR Registry. Ann Rheum Dis 2004;63:974-81.
10. de Buys P, Khanna D, Furst DE. Hemopoietic stem cell transplantation in rheumatic diseases—an update. Autoimmun Rev 2005;4:442-9.
11. Endo T, Sato N, Koizumi K, et al. A preliminary analysis of the balance between Th1 and Th2 cells after CD34+ cell-selected autologous PBSC transplantation. Cytotherapy 2004;6:337-43.
12. Moore J, Brooks P, Milliken S, et al. A pilot randomized trial comparing CD34-selected versus unmanipulated hemopoietic stem cell transplantation for severe, refractory rheumatoid arthritis. Arthritis Rheum 2002;46:2301-9.
13. Farge D, Marolleau JP, Zohar S, et al. Autologous bone marrow transplantation in the treatment of refractory systemic sclerosis: early results from a French multicentre phase I-II study. Br J Haematol 2002;119:726-39.
14. Traynor AE, Schroeder J, Rosa RM, et al. Treatment of severe systemic lupus erythematosus with high-dose chemotherapy and haemopoietic stem-cell transplantation: a phase I study. Lancet 2000;356:701-7.
15. Muraro PA, Douek DC, Packer A, et al. Thymic output generates a new and diverse TCR repertoire after autologous stem cell transplantation in multiple sclerosis patients. J Exp Med 2005;20:805-16.
16. Preliminary criteria for the classification of systemic sclerosis (scleroderma). Subcommittee for scleroderma criteria of the American Rheumatism Association Diagnostic and Therapeutic Criteria Committee. Arthritis Rheum 1980;23:581-90.
17. Douek DC, Vescio RA, Betts MR, et al. Assessment of thymic output in adults after haematopoietic stem-cell transplantation and prediction of T-cell reconstitution. Lancet 2000;355:1875-81.
18. Farge D, Henegar C, Carmagnat M, et al. Analysis of immune reconstitution after autologous bone marrow transplantation in systemic sclerosis. Arthritis Rheum 2005;52:1555-63.
19. Hori S, Nomura T, Sakaguchi S. Control of regulatory T cell development by the transcription factor Foxp3. Science 2003;299:1057-61.
20. Steen VD, Medsger TA, Jr. Improvement in skin thickening in systemic sclerosis associated with improved survival. Arthritis Rheum 2001;44:2828-35.
21. McSweeney PA, Nash RA, Sullivan KM, et al. High-dose immunosuppressive therapy for severe systemic sclerosis: initial outcomes. Blood 2002;100:1602-10.
22. Douek DC, McFarland RD, Keiser PH, et al. Changes in thymic function with age and during the treatment of HIV infection. Nature 1998;396:690-5.
23. Vieira QF, Kayser C, Kallas EG, Andrade LE. Decreased recent thymus emigrant number is associated with disease activity in systemic lupus erythematosus. J Rheumatol 2008;35:1762-7.
24. Prelog M, Schwarzenbrunner N, Sailer-Hock M, et al. Premature aging of the immune system in children with juvenile idiopathic arthritis. Arthritis Rheum 2008;58:2153-62.
25. Hakim FT, Memon SA, Cepeda R, et al. Age-dependent incidence, time course, and consequences of thymic renewal in adults. J Clin Invest 2005;115:930-9.
26. Williams KM, Hakim FT, Gress RE. T cell immune reconstitution

Bohgaki, et al: Autologous HSCT in SSc

following lymphodepletion. Semin Immunol 2007;19:318-30.

27. Muraro PA, Douek DC. Renewing the T cell repertoire to arrest autoimmune aggression. Trends Immunol 2006;27:61-7.
28. Guillaume T, Rubinstein DB, Symann M. Immune reconstitution and immunotherapy after autologous hematopoietic stem cell transplantation. Blood 1998;92:1471-90.
29. Damiani D, Stocchi R, Masolini P, et al. CD34+-selected versus unmanipulated autologous stem cell transplantation in multiple myeloma: impact on dendritic and immune recovery and on complications due to infection. Ann Oncol 2003;14:475-80.
30. Te Boekhorst PA, Lamers CH, Schipperus MR, et al. T-lymphocyte reconstitution following rigorously T-cell-depleted versus unmodified autologous stem cell transplants. Bone Marrow Transplant 2006;37:763-72.
31. de Kleer I, Vastert B, Klein M, et al. Autologous stem cell transplantation for autoimmunity induces immunologic self-tolerance by reprogramming autoreactive T cells and restoring the CD4+CD25+ immune regulatory network. Blood 2006;107:1696-702.
32. Roncarolo MG, Battaglia M. Regulatory T-cell immunotherapy for tolerance to self antigens and alloantigens in humans. Nat Rev Immunol 2007;7:585-98.
33. Bohgaki T, Atsumi T, Koike T. Multiple Autoimmune Diseases after Autologous Stem-Cell Transplantation. N Engl J Med 2007;357:2734-6.
34. Loh Y, Oyama Y, Statkute L, et al. Development of a secondary autoimmune disorder after hematopoietic stem cell transplantation for autoimmune diseases: role of conditioning regimen used. Blood 2007;109:2643-548.

Collagen XVII Participates in Keratinocyte Adhesion to Collagen IV, and in p38MAPK-Dependent Migration and Cell Signaling

Hongjiang Qiao[1,2,3], Akihiko Shibaki[2,3], Heather A. Long[2], Gang Wang[2], Qiang Li[2], Wataru Nishie[2], Riichiro Abe[2], Masashi Akiyama[2], Hiroshi Shimizu[2] and James R. McMillan[1,2]

Collagen XVII (COL17) participates in keratinocyte adhesion and possibly migration, as COL17 defects disrupt keratinocyte-basal lamina adhesion and underlie the disease non-Herlitz junctional epidermolysis bullosa. Using small interference RNA (siRNA) to knock down COL17 expression in HaCaT cells, we assessed cell characteristics, including adhesion, migration, and signaling. Control and siRNA-transfected keratinocytes showed no difference in adhesion on plastic dishes after incubation for 8 hours in serum-free keratinocyte-growth medium; however, when grown on collagen IV alone or BD matrigel (containing collagen IV and laminin isoforms), COL17-deficient cells showed significantly reduced adhesion compared with controls ($P<0.01$), and mitogen-activated protein kinase (MAPK)/ERK kinase (MEK)1/2 and MAPK showed reduced phosphorylation. Furthermore, COL17-deficient HaCaT cells plated on plastic exhibited reduced motility that was p38MAPK-dependent (after addition of the p38MAPK inhibitor SB203580). Together, these results suggest that COL17 has significantly wider signaling roles than were previously thought, including the involvement of COL17 in keratinocyte adhesion to collagen IV, in p38MAPK-dependent cell migration, and multiple cell signaling events pertaining to MEK1/2 phosphorylation.

INTRODUCTION

Collagen XVII (formerly known as BPAG2 or BP180) (COL17) is a transmembrane protein that plays a critical role in linking the cytoskeleton and the extracellular environment (Shimizu et al., 1989; Franzke et al., 2005). It is also an autoantigen in bullous pemphigoid, a blistering skin disease (Jablonska et al., 1958; Sams, 1970; Shimizu et al., 1989). Mutations in the human COL17 gene, COL17A1, lead to COL17 protein deficiency, reduced keratinocyte-basement membrane adhesion, and reductions in the size of hemidesmosome (HD) plaques, involved in epidermal adhesion (McMillan et al., 1998) (Zillikens and Giudice, 1999). These defects lead to non-Herlitz junctional epidermolysis bullosa, an autosomal recessive blistering disease with a variable clinical phenotype

largely dependent on mutation severity (McGrath et al., 1995, 1996; Bauer and Lanschuetzer, 2003).

Epidermal keratinocytes expressing defective COL17 show altered basement-membrane adhesion, increased skin separation (Nakamura et al., 2006; Nishie et al., 2007), and increased migration rates (Tasanen et al., 2004). COL17-knockout mice (Nishie et al., 2007) show a similar phenotype to that of nHJEB patients, including multiple erosions and hair defects and premature loss of hair (McGrath et al., 1995, 1996; Bauer and Lanschuetzer, 2003).

Regulation of keratinocyte adhesion and migration likely involves COL17 collagenous ectodomain shedding because of cleavage close to the plasma membrane of keratinocytes and malignant epithelial cells (Franzke et al., 2002, 2004; Labrousse et al., 2002; Zimina et al., 2005, 2007). The shed ectodomain is thought to regulate attachment by inducing cell detachment, profoundly affecting cell adhesion and subsequent signaling, thereby increasing motility, and disrupting differentiation, and it is already known to be involved in autoimmune disease development (Schumann et al., 2000).

The process of cell migration over the extracellular matrix plays a critical role not only in maintaining epidermal homeostasis but also in promoting angiogenesis, and it is involved in inflammation, embryonic development (Martin and Parkhurst, 2004), wound repair (Friedl, 2004; Friedl et al., 2004), and tumor metastasis (Braiman-Wiksman et al.,

[1]Creative Research Initiative, Hokkaido University, Sapporo, Japan and [2]Department of Dermatology, Hokkaido University Graduate School of Medicine, Sapporo, Japan

[3]These authors contributed equally to this work

Correspondence: Dr James R. McMillan, Department of Dermatology, Hokkaido University Graduate School of Medicine, North 15 West 7, Kitaku, Sapporo 060-8638, Japan. E-mail: jrm57@med.hokudai.ac.jp

2007; Raja *et al.*, 2007). Central to this process, several papers have reported that activation of the mitogen-activated protein kinase (MAPK) pathway leads to transcriptional control of genes important for cell proliferation and differentiation (Zhang *et al.*, 2004; Deng *et al.*, 2006; Choma *et al.*, 2007). However, both growth factor receptors and integrins can also induce multiple signaling events leading to MAPK activity and the rapid induction of cell migration, suggesting that MAPK can lead to direct activation of the intracellular motility machinery independent of *de novo* gene transcription. (Pearson *et al.*, 2001; Stoll *et al.*, 2003; Deng *et al.*, 2006; Fitsialos *et al.*, 2007).

In this study, we analyzed the precise mechanism(s) whereby COL17 modulates keratinocyte migration under various physiological and pathological situations to gain a better understanding of the general role of COL17 in the regulation of keratinocyte adhesion, signaling activation, and p38MAPK-dependent migration.

RESULTS

Establishment of COL17-knockdown clones

In an effort to determine whether expression of COL17 in HaCaT cells can affect cell characteristics such as cell motility and morphology, we used RNA interference approaches to knock down COL17 expression. First, HaCaT cells were transfected using lipofectamine with the plasmid-based vector pSilencer 3.0-hygro, specific to human COL17 or to green fluorescent protein (GFP), and clones were selected using 0.4 mg/ml hygromycin. To confirm the extent of COL17-expression knockdown in subcloned cell lines (si17-4 and -6; N. C., respectively *vs* controls), total RNA and protein were harvested and analyzed by RT-PCR and western blotting. COL17 gene expression studied by RT-PCR (Figure 1a) showed a marked reduction in the relative ratio of COL17 expression to the glyceraldehyde-3-phosphate dehy-drogenase housekeeping gene internal control. These data show an approximate fourfold reduction in COL17 message expression in comparison with the control cells. Western blotting data showed similar reductions in both mRNA and protein expression. The blotting results, shown in Figure 1b, showed a significantly reduced level of COL17 in cells that had been transfected with the two vectors expressing short hairpin RNA against COL17 (pSi-COL17). The levels were significantly lower than those in wild type or control short hairpin RNA (pSi-GFP) transfected-HaCaT cells, without any detectable change in *β*-actin expression. Densitometry scanning to quantify the western blots revealed the degree of protein expression to be about 70% of control COL17 protein levels, whereas the siGFP-treated cells failed to show any significant change in COL17 expression. All cell lines showed no changes in cell viability compared with wild-type HaCaT cells (data not shown).

COL17-knockdown HaCaT cells show reduced motility but no change in adhesion

To study the role of COL17 in the migration of cells plated onto uncoated plastic dishes, cells were incubated in serum-free keratinocyte-growth medium at 37 °C for 8 hours
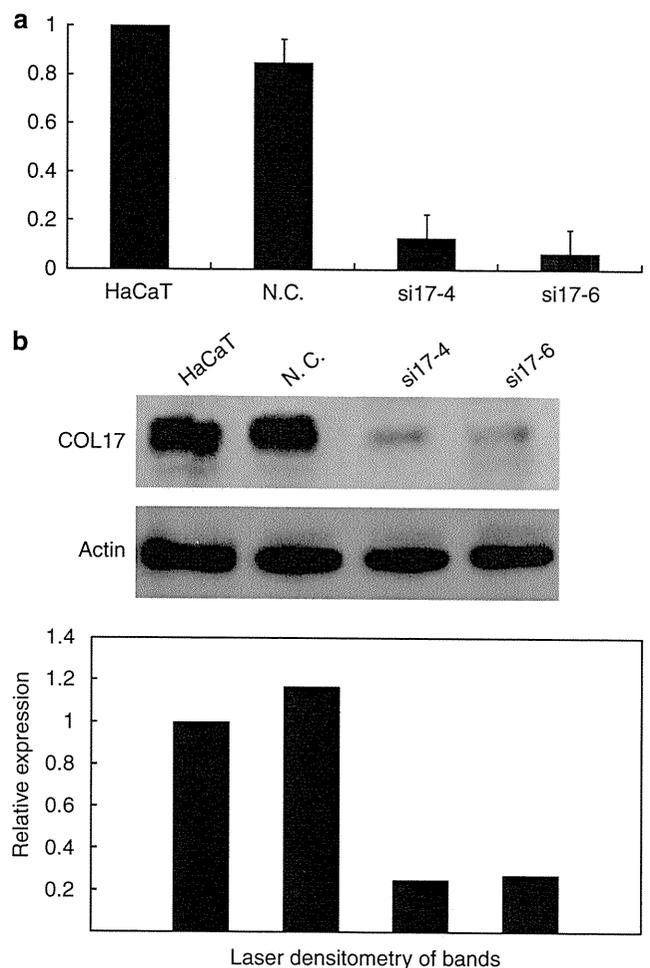

Figure 1. **Expression of COL17 in HaCaT cell lines and COL17-knockdown clones by RT-PCR and immunoblot analysis.** (a) RT-PCR studies of reference RT-RNA samples validated decreased expression of COL17 (by approximately fourfold) in si17-4 and si17-6 cell lines compared with normal and mock-transfected controls. HaCaT: parental cells; N. C.: GFP siRNA vector-transfected HaCaT cells; si17-4 and -6: COL17 siRNA-expressed clones. Three experiments were performed in duplicate, and values represent the mean + SE. (b) Confirmation of stable expression of COL17 in the HaCaT cell line. The expression of actin was monitored to ensure equivalent loading and protein transfer.

(calcium concentration at 0.2 or 1.44 mM). Subconfluent cells were seeded, and after 2 hours the distance (in μm) migrated by the cells was measured using ImageJ software (Figure 2a). Compared with COL17-knockdown clones, HaCaT cells and negative-control cell line cells migrated approximately 2- to 2.5-fold further during the ensuing 12-hour period (Figure 2b). The addition of keratinocyte growth factor to the medium increased the migration rates in control HaCaT cells and COL17-knockdown cells (Figure 2b). These findings suggest that untreated or control GFP-transfected HaCaT cells are more motile than COL17-knockdown cells when plated on uncoated tissue culture plastic (TCP) dishes. We then compared the adhesion of HaCaT cells to COL17-knockdown siRNA-treated HaCaT cells in a short-term adhesion assay on uncoated dishes. The adhesion of siRNA-treated HaCaT cells was equivalent to that of HaCaT cells on uncoated dishes
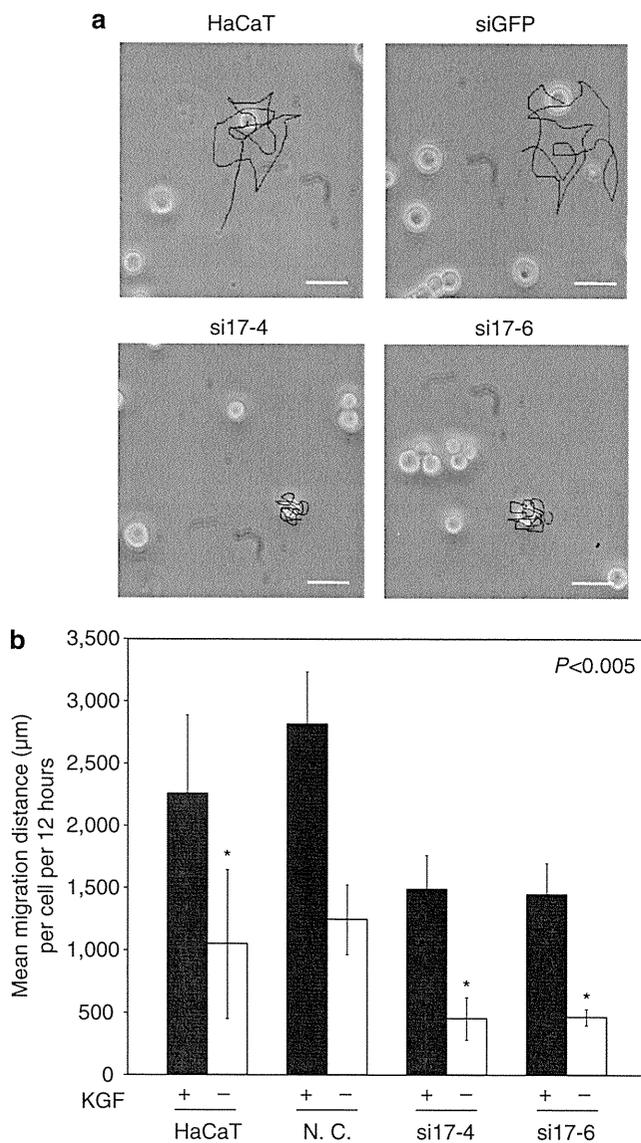
Figure 3. **Cell adhesion and migration assays on collagen I, IV or BD-matrigel coated dishes.** (a) The results showed no differences in adhesion in the control and COL17-deficient cells on uncoated tissue culture plastic, but significant reductions in the number of COL17 deficient cells attached ($P<0.005$) on collagen IV and BD-Matrigel substrate. Collagen I-coated dishes showed only minor and statistically insignificant changes in adhesive cell number between control and COL17-deficient cells. (b) Cell migration distance was also checked under the same conditions as adhesion. Similar results were obtained with cells on uncoated plastic dishes with COL17-knockdown cells showing reduced migration rates on all three substrates compared with controls. Migration of COL17-knockdown cells showed slightly larger reductions compared with controls when grown on collagen IV and BD-Matrigel substrate. Three experiments were performed in duplicate, and values represent the mean + SE.

Figure 2. **Cell migration of control and COL17 knockdown HaCaT-derived cell lines.** (a) Representative cell tracks of control and siRNA-treated cells, scale bar: 100 μm. The distance (in μm) migrated by the cells was measured using ImageJ software. (b) Assessment of total cell migration distance over 12 hours showed that control and GFP-transfected HaCaT cell lines both showed high migration rates, but the two COL17-knockdown cell lines showed dramatically reduced rates of cell migration (by more than twofold) on uncoated tissue culture plastic. KGF was added into HaCaT cells and COL17-knockdown cells as positive control for assessing migration potential. Three experiments were performed in duplicate, and values represent the mean + SE.

(Figure 3a). Thus, COL17 is involved in regulating normal migration of HaCaT cells on uncoated TCP dishes, but is not involved in HaCaT cell attachment to uncoated TCP. To analyze the role of COL17 in adhesion, cells were plated onto dishes coated with different proteins, collagen types I, IV, and BD-Matrigel. The adhesion of COL17 knockdown HaCaT cells was significantly reduced ($P<0.005$) compared with that of control HaCaT cells on collagen IV and BD-Matrigel-coated dishes (BD-Matrigel comprises both collagen IV and multiple laminin isoform chains) (Figure 3a). Furthermore, the
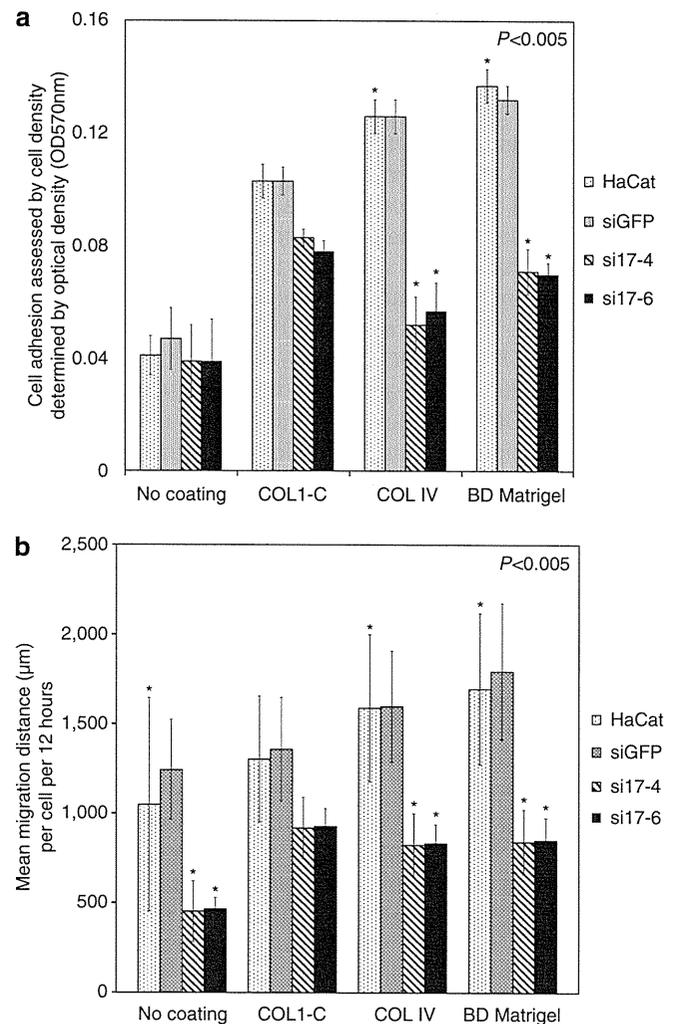
extent to which adhesion was reduced was roughly equivalent in both collagen and Matrigel-coated dishes. We surmise that COL17 is important in cell adhesion to collagen IV, and a similar effect can be seen with the collagen IV present in the BD-Matrigel-coated dishes. However, COL17-depleted cells showed only marginally weaker binding to collagen I and is therefore likely to be less important in cultured cell adhesion to collagen I. The migration of these cells on different substrates was also investigated. Similar to the results shown on uncoated TCP dishes, HaCaT cells and GFP-transfected

-288-

control cells migrated approximately twofold farther compared with COL17-knockdown clones over 12 hours when plated on collagen IV or Matrigel-coated dishes (Figure 3b). In addition, COL17-knockdown HaCaT cells plated on collagen I coated dishes showed marginal reductions in motility, although the difference was not statistically significant.

Activation of MAPK in HaCaT cells

Earlier reports have implicated the involvement of MAPK activity in cell motility (Stoll *et al.*, 2003; Choma *et al.*, 2007; Fitsialos *et al.*, 2007). We therefore used siRNA-transfected HaCaT cells to investigate the role of MAPK in COL17-regulated cell motility. The activation of MAPK was measured by antiphosphotyrosine immunoblotting. Compared with the untreated HaCaT cells cultured in keratinocyte-growth medium, siRNA-treated COL17-knockdown HaCaT cells showed reduced MAPK/ERK kinase (MEK) 1/2 activity (Figure 4). It is known that activated MEK1/2 can activate p38MAPK (Slack-Davis *et al.*, 2003; Manohar *et al.*, 2004; Deng *et al.*, 2006), and this is thought to be important in the regulation of keratinocyte migration. We therefore examined whether siRNA treatment downregulates p38MAPK activity in HaCaT keratinocytes (Figure 4). siRNA-induced COL17 knockdown reduced p38MAPK activity in HaCaT cells. In contrast, the total amount of both MEK 1/2 and p38MAPK was not changed by siRNA-induced COL17 knockdown. These results indicate that COL17 knockdown reduced MAPK activity, possibly resulting in reduced HaCaT cell migration.

MAPK inhibitors inhibit COL17-regulated cell migration but not adhesion

To further analyze the role of p38MAPK activation in the control of keratinocyte migration, we next investigated whether inhibition of the p38MAPK pathways could prevent

the regulation of cell migration by COL17. Pretreatment of cells with the p38MAPK inhibitor SB 203580 blocked cell migration in a dose-dependent manner and also blocked the activation of p38MAP (Figure 5a). The 10 μM dose was selected as the lowest optimal dose of SB 203580 to be used in these inhibition of migration experiments. Pretreatment of cells with 10 μM SB 203580 inhibited cell migration by approximately 60% compared with untreated cells (Figure 5b). Under identical conditions, adhesion was again measured and the p38 inhibitor SB 203580 failed to show any effect on cell adhesion (Figure 5c). These data show that MAPK-inhibitors inhibit COL17-dependent cell migration but not adhesion, and therefore p38MAPK activation is important for migration but not adhesion in keratinocyte culture systems.

DISCUSSION

COL17 is a HD component that is involved in HD-attachment plaque stability and in providing basal-keratinocyte adhesion to the underlying epidermal basement membrane and extracellular matrix (McGrath *et al.*, 1995; McMillan *et al.*, 1998; Nishie *et al.*, 2007). Defects in keratinocyte COL17 expression have marked consequences on cell behavior, as earlier papers have reported that COL17 deficiency induces a migratory phenotype (Tasanen *et al.*, 2004; Zimina *et al.*, 2005). *In vivo*, HDs are associated with stable keratinocyte anchorage, and conversely, HD disassembly is a prerequisite for keratinocyte migration (De Luca *et al.*, 1994; Poumay *et al.*, 1994; Raja *et al.*, 2007). Thus, the integration of COL17 in the keratinocyte attachment complex represents an important step in the sequence of events regulating robust keratinocyte adhesion, limiting migration, and our results show that siRNA COL17 knockdown affects cell migration and adhesion on collagen IV and Matrigel substrates. Interestingly, siRNA COL17 knockdown of HaCaT cells on TCP showed a reduced migratory phenotype that contradicts other studies. Tasanen *et al.* reported that keratinocytes with COL17 null mutations showed increased cell migration compared with wild-type cells (Tasanen *et al.*, 2004). However, they studied human junctional epidermolysis bullosa patient keratinocytes with COL17 null mutations and used laminin 332 (laminin 5)-coated substrates that affect keratinocyte adhesion in a different manner, and thus explain the different findings. BD-Matrigel contains mouse laminin isoforms (including laminin 111, formerly laminin 1, and likely several other isoforms) and siRNA COL17-depleted HaCaT cells exhibited reduced adhesion, which may allow for the more motile environment shown in earlier reports. The involvement of COL17 in cell migration has been shown earlier(Tasanen *et al.*, 2004; Parikka *et al.*, 2006; Huilaja *et al.*, 2007). An optimum level of adhesion strength is generally thought to be required for cell migration, suggesting that markedly weak adhesion may also impair proper cell traction. Similarly, excessive adhesion can also inhibit motility, and therefore precise and correct control of cell dysadhesion is required for optimal migration rates. The role of COL17 in the stabilization of epithelial cells on various matrices *in vitro* provides an explanation for the lack of
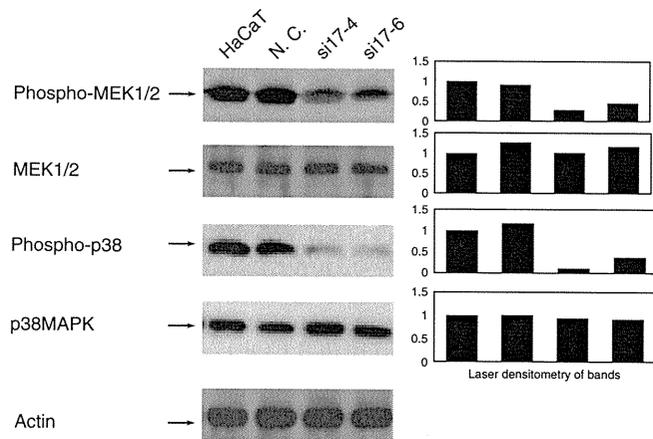

Figure 4. Laser densitometry analysis of protein immunoblots from control and COL17-deficient HaCaT-derived cell lines. Laser densitometry showed that both phospho-MEK1/2 and phospho-p38 MAPK showed reduced immunostaining in COL17-deficient cell lines. These results showed that MEK1/2 and MAP kinase activation is greater in untreated HaCaT cells than in siRNA COL17-knockdown HaCaT cells. We observed no change in MEK1/2 and p38MAPK, and there was normal staining of equal intensity for the unphosphorylated forms of MEK1/2 and p38MAPK. The expression of actin was used as an internal standard loading and protein transfer control.
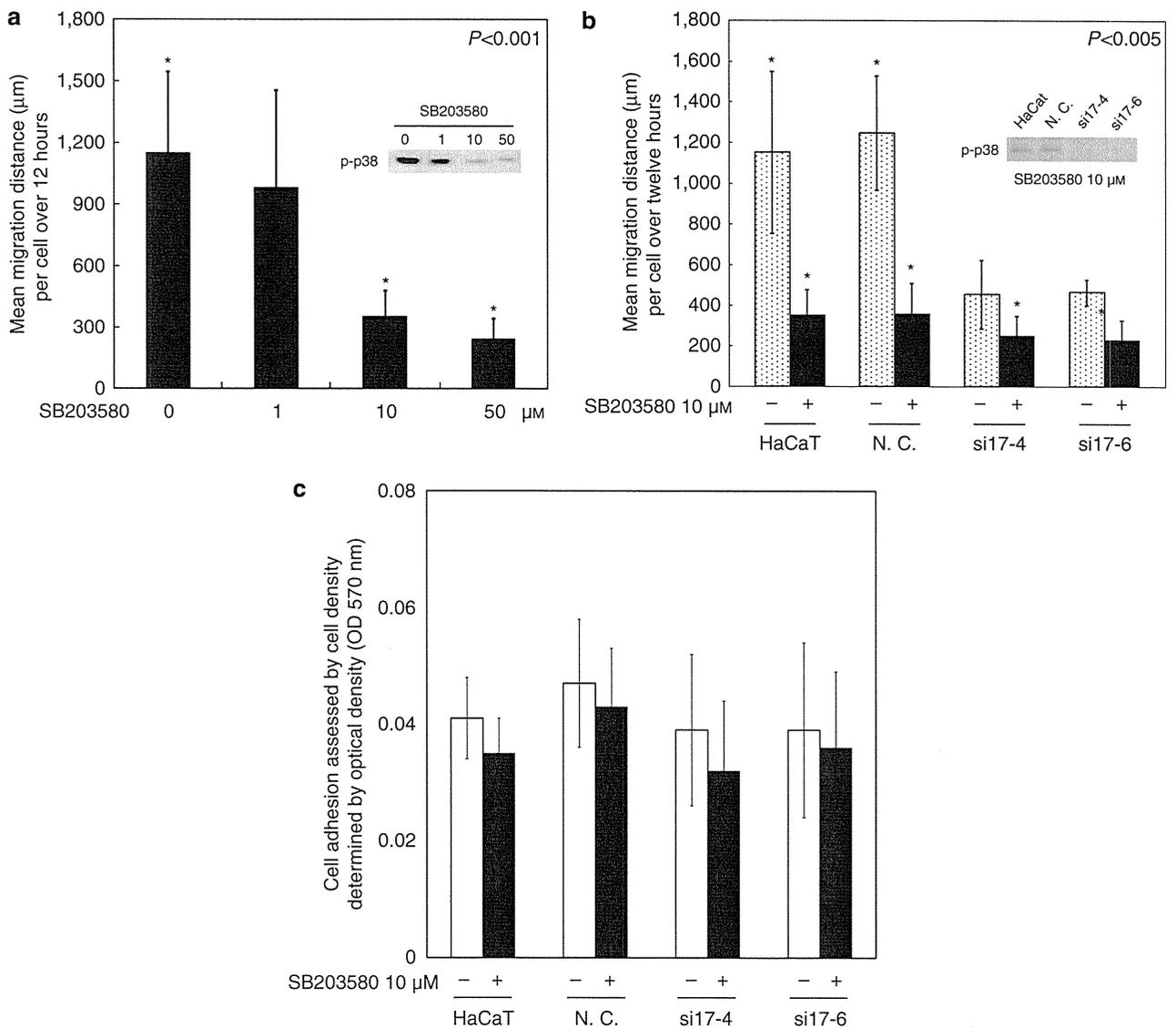
Figure 5. SB 203580 inhibits COL17-regulated cell migration but not adhesion. Inhibition of keratinocyte migration by the MAPK inhibitor SB 203580 (a) is dose-dependent, (b) but does not rely on normal COL17 levels of expression. Dose response of MAPK inhibitor SB 203580 shows a significant reduction in keratinocyte motility at levels above 10 μM (this value was then used in subsequent experiments to determine the role of MAPK in COL17-deficient migration suppression). Both COL17-deficient HaCaT cells and MAPK inhibition using SB 203580 suppressed keratinocyte migration to a similar extent, but (b) without any synergistic effect, and (c) this inhibitor did not affect adhesion in any cell line. Results of western blotting, which show phosphorylation status of p38 in each condition, three experiments were performed in duplicate, and values represent the mean + SE.

keratinocyte adhesion to the dermal-epidermal junction in COL17-deficient nHJEB patients. Indeed, patients lacking COL17 do exhibit a relatively mild blistering phenotype because of their lack of robust adhesion to the basal lamina extracellular matrix components that likely include the collagens (particularly collagen IV), α6β4 integrin, or laminin 332. COL17 is expressed in the upper part of the outer root sheath hair follicle keratinocytes (Messenger *et al.*, 1991; Joubeh *et al.*, 2003) and in ameloblast cells involved in tooth formation, consistent with nHJEB patients exhibiting associated hair and tooth defects. Cell adhesion and migration are generally thought to be critical for the maintenance of the keratinocyte hair follicle bulge population and interfollicular regions, and thus loss of COL17 and subsequent effects on

cell adhesion, migration, and signaling during the hair cycle and differentiation in these regions explain the hair loss and skin thinning observed in nHJEB COL17-deficient patients.

Cell migration requires a complex coordinated interaction of proteins and signaling events that control important cell motility events. Our results show that COL17 siRNA knockdown affects cell migration through the p38MAPK-signaling pathway. The MAPK pathway influences many cellular processes, including cell division, gene transcription, and stress responses. Many papers have reported the role of MAPK in cell migration, acting on cytoskeletal components (Osmanagic-Myers *et al.*, 2006; Pullikuth and Catling, 2007). MAPK signaling events have been shown to be triggered by a number of different growth factors, cytokines, and integrins,

which influence specific cell migration events. Cellular transformation by H-Ras or c-Src is also associated with increased MAPK activity and enhanced cell proliferation, and migration in neoplasia. The MAPK pathways are involved not only in cell migration but also in aspects of cell adhesion (integrin attachment initiates downstream signaling). In this report, we provide evidence that p38MAPK signaling can regulate cell migration by directly affecting the migratory machinery. Blocking p38MAPK activity with a selective inhibitor resulted in the loss of cell migration, with no obvious effect on cell adhesion. Our results suggest that COL17 may be involved in p38MAPK-signaling pathways during cell migration, but that it is not a prerequisite for *in vitro* adhesion, suggesting mutually exclusive p38MAPK-signaling pathways involving COL17 adhesion and migration. The precise relationship between COL17 and p38MAPK in cell migration is not yet clear: whether it is a direct interaction or acts through other secondary factors. The MAPK pathway cross talks with many different signaling pathways to regulate cellular activities and likewise other signaling molecules can influence upstream and downstream targets of the p38MAPK pathway, which allows fine control of specific cellular activities. With ongoing investigation, the interactions of p38MAPK and COL17 with other signaling pathways can be clarified.

A further important finding was that cells with normal levels of COL17 showed higher rates of adhesion to collagen IV or BD-Matrigel (comprising mouse laminin isoforms and collagen IV) than to collagen I or plastic in comparison. From our data, we hypothesize that COL17 may play a specific role in collagen IV adhesion, albeit with weaker association in comparison to laminin 332-integrin α6β4 adhesive interaction. Such interactions fit with the clinically milder phenotype observed in non-Herlitz junctional epidermolysis bullosa human patients and mouse models.

Taken together, our data suggest that keratinocyte adhesion and migration are differentially regulated. This is the case as many different adherent cell types do not migrate without prior specific cytokine or growth factor stimulation. Earlier studies have shown that MAPK activity is critical for transcriptional gene events leading to cell proliferation and differentiation, which may explain how COL17 and MAPK activation can independently influence cell movement on different extracellular matrices during tissue remodeling, as well as tumor cell invasion. Our findings suggest that COL17 is important in keratinocyte adhesion and in relaying signals from the extracellular matrix to the internal signaling apparatus during cell migration.

MATERIALS AND METHODS
Cell culture and establishment of stable cell lines
The HaCaT cell line (Boukamp *et al.*, 1990), a spontaneously transformed but non-malignant human keratinocyte cell line, was used in this study. The cells were cultured at 37 °C in a 5% CO_2 humidified atmosphere in Dulbecco's modified Eagle's medium (DMEM) containing 10% fetal calf serum (Gibco BRL, Gaithersburg, MD). HaCaT cells were passaged overnight at a concentration of 5×10^4/ml to 1×10^5/ml, in 6-well plates under standard conditions.

Fifteen-minutes before transfection, the medium was changed to OPTI-MEM (Gibco Invitrogen, Carlsbad, CA) quiescent medium (without fetal calf serum). Transfections were carried out using Lipofectamine transfection reagent (Invitrogen, Carlsbad, CA) according to the manufacturer's instructions. Four hours after transfection, medium containing 10% fetal calf serum was added. Two stable monoclonal lines from the single cell of siRNA expression vector transfectants (si17-4, si17-6) were established after medium treatment with 0.3 mg/ml hygromycin (Wako, Osaka, Japan) for 7 days, using limiting dilution methods. The relative reduction in COL17 expression by siRNA was analyzed by immunoblotting cell culture extracts and RT-PCR.

RNA interference (I)
We designed small interference siRNA nucleotides to knock down COL17 expression as described in the manufacturer's technical information (Ambion, Austin, TX). A set of 19-mer oligonucleotides (AAGTATTGCTGTCAAGCCGTG), corresponding to 4,642 nucleotides downstream of the transcription start site, was selected. We confirmed that the selected oligonucleotide sets failed to show homology to any other genes by BLAST searching and that they would not therefore interfere with other genes. The oligonucleotides were synthesized and column purified. The 19-mer sense siRNA sequence and antisense siRNA sequences were linked with a nine nucleotide spacer (TTCAAGAGA) loop. Six T bases and 6 A bases were added as a termination signal to the 3' end of the forward oligonucleotides and the 5' end of the reverse oligonucleotides, respectively. Five nucleotides corresponding to the Bam HI (GATCC) and Hind III (AGCTT) restriction sites were then added to the 5' end of the forward oligonucleotides and the 3' end of the reverse oligonucleotides, respectively. Forward and reverse oligonucleotides were incubated in annealing buffer (100 mM K-acetate, 30 mM HEPESKOH (pH 7.4), and 2 mM Mg-acetate) for 3 minutes at 90 °C, followed by incubation for 1 hour at 37 °C. The annealed DNA fragment was ligated with the linearized pSilencer 3.1-H1 hygro siRNA plasmid expression vector (Ambion) at the Bam HI and Hind III sites, and a COL17 siRNA vector (pSi-COL17) was thus constructed. A negative-control siRNA vector (pSi-GFP) that targeted using an unrelated (non-specific) GFP cDNA sequence 5'-GGTTATGTACAGGAACGCA-3' that had no matches to any human gene was also prepared under similar conditions.

RNA extraction and quantification using RT-PCR
Total RNA was extracted from HaCaT cells using TRIzol (Invitrogen, Burlington, ON, Canada). RNA was dissolved in 30 DEPC-H_2O and immediately stored at −70 °C. The concentration and purity of RNA were evaluated by measuring the absorbance at 260 nm, and by calculating the ratio of absorbance at 260–280 nm using a UV spectrophotometer (Ultrospec-3000 spectrophotometer, Pharmacia Biotech, UK). RT-PCR analysis for COL17 was performed on RNA extracts using ABI prism 7500 (Applied Biosystems, Foster City, CA) and the 5'exonuclease assay (TaqMan technology). The cDNA was used for RT-PCR performed in 96-well optical reaction plates with cDNA equivalent to 30 ng RNA in a reaction of 25 μl containing 1X Taqman Universal Master Mix, 900 nM of specific forward and reverse primer for COL17. Controls included RNA subjected to RT-PCR without reverse transcriptase and PCR with water replacing cDNA template. The data were normalized using glyceraldehyde-3-

phosphate dehydrogenase mRNA expression levels as an internal standard, and converted into fold change on the basis of a doubling of PCR product in each PCR cycle, according to the manufacturer's guidelines described earlier.

Analysis of migration assay

The effects of COL17 on cell migration were studied using 3 cm plastic coated dishes. HaCaT cells were incubated in serum-free keratinocyte growth medium (Cambrex, Walkersville, MD) at 37 °C for 8 hours. HaCaT cells in logarithmic-growth phase were detached using trypsin–EDTA. In all, 3,000 cells were seeded in 3 cm TCP dishes and further cultured at 37 °C in a 5% CO_2 humidified atmosphere in serum-free DMEM. Migrating cells were photographed every 5 minutes using time-lapse video (Olympus DP70, Tokyo, Japan) from 2–14 hours after plating. The distance migrated by 40 cells over 12 hours was later measured using ImageJ software (McMillan *et al.*, 2007). To analyze the migration on dishes coated with different proteins, 50 µl cell matrix type I (2.4 mg/ml), type IV collagens (2.4 mg/ml) (Nitta Gelatin, Osaka, Japan), and 50 µl BD Matrigel (10.0–12.0 mg/ml) (BD Bioscience, San Jose, CA) were coated on petri dishes according to the manufacturer's protocol. After drying, multiwell tissue culture plates were washed in serum-free DMEM and then used immediately for cell migration assays. For MAPK inhibition experiments, a p38MAPK specific inhibitor (SB 203580) (Hornby, ON, Canada) was purchased from Calbiochem and used at a final concentration of 10 µM after dose optimization, and was added to serum-free medium. At the same time, 0.5 nM keratinocyte growth factor (NIBSC, Hertfordshire, UK) was used as positive control for migration assays (Ceccarelli *et al.*, 2007).

Cell adhesion assays

To analyze adhesion, 96-well plates were used. Wells were rinsed with phosphate-buffered saline (PBS) and blocked with 0.1% BSA in PBS for 30 minutes before use. HaCaT cells in serum-free DMEM containing 0.1% BSA were seeded at a concentration of 5×10^4 cells/well. After 1 hour at 37 °C, cells were rinsed twice with PBS, fixed for 10 minutes at room temperature in 70% ethanol, rinsed again with PBS and stained in 0.1% crystal violet (Tokyo Chemical Industry, Tokyo, Japan), and kept in water for 30 minutes at room temperature. After staining, cells were rinsed 3 times with water, air dried, and solubilized in 1% SDS in PBS, and the OD color read with an ELISA-plate reader (Mithras LB 940, Berthold Inc., Tokyo, Japan) at 570 nm. A blank value corresponding to BSA-coated wells was automatically subtracted. To analyze adhesion on dishes coated with different proteins, cell matrix type I and type IV collagens, BD-Matrigel was coated to the dishes using the same method as described above. After drying, multiwell tissue culture plates were washed in serum-free DMEM, then immediately used for cell adhesion assays as described above.

Activation of MEK1/2 and p38MAPK

Cells were incubated in serum-free keratinocyte-growth medium at 37 °C for 8 hours. Cells were solubilized in SDS-sample buffer (40 mM Tris-HCl, pH 7.4, 5% 2ME, 2% SDS, 0.05% bromphenol blue), and the cell extracts were subjected to western immunoblotting analyses using either anti-phospho-MEK1/2 antibody (166F8) or anti-phospho-p38MAPK antibody (12F8), which selectively recognizes the activated forms of MEK1/2 (phosphorylated Ser 221) or p38MAPKs (phosphorylated Thr180/Tyr182), respectively. To detect MEK1/2 or p38MAPKs, anti-MEK1/2 antibody or anti-p38MAPK antibody was used. All of these antibodies were purchased from Cell Signaling (Danvers, MA). Actin was used as the loading control to account for equal protein loading for each blot lane. For these experiments, equal amounts of cell extract (>50 mg of total proteins) were resolved on an SDS polyacrylamide gel, transferred to a nitrocellulose membrane (Bio-Rad Laboratories, Inc., Tokyo, Japan), and immunoblotted with corresponding antibodies. The results were visualized by a horseradish-peroxidase-conjugated secondary antibody.

Immunoblotting analysis

Total cell cultures were extracted using lysis buffer as described earlier. Cell lysates were analyzed by SDS-polyacrylamide gel electrophoresis and blotted as described earlier, using goat anti-COL17 (*N*-18) polyclonal antibody (Santa Cruz, CA), anti-MEK1/2 monoclonal antibody, and anti-phospho-MEK1/2, anti-p38MAPK and phospho-p38MAPK (Cell Signaling, Danvers, MA), and anti-β-actin monoclonal antibody (Chemicon, Temecula, CA). The bound primary antibodies on membranes were incubated with peroxidase-conjugated anti-mouse IgG + M (Jackson ImmunoResearch Lab., West Grove, PA) or anti-goat IgG (R&D Systems, Inc., Minneapolis, MN) and detected by enhanced chemiluminesence western blotting detection reagents (Amersham Biosciences, Amersham, UK). Band images were detected by an LAS 1000 mini system (Fuji Film, Kanagawa, Japan).

Statistical analysis

The data shown represent mean values of at least three different experiments, expressed as mean ± SE. Student's *t*-test was used to compare the data, and a *P*-value of <0.05 was considered to be statistically significant.

REFERENCES

Bauer JW, Lanschuetzer C (2003) Type XVII collagen gene mutations in junctional epidermolysis bullosa and prospects for gene therapy. *Clin Exp Dermatol* 28:53–60

Boukamp P, Stanbridge EJ, Foo DY, Cerutti PA, Fusenig NE (1990) c-Ha-ras oncogene expression in immortalized human keratinocytes (HaCaT) alters growth potential *in vivo* but lacks correlation with malignancy. *Cancer Res* 50:2840–7

Braiman-Wiksman L, Solomonik I, Spira R, Tennenbaum T (2007) Novel insights into wound healing sequence of events. *Toxicol Pathol* 35:767–79

Ceccarelli S, Cardinali G, Aspite N, Picardo M, Marchese C, Torrisi MR *et al.* (2007) Cortactin involvement in the keratinocyte growth factor and fibroblast growth factor 10 promotion of migration and cortical actin assembly in human keratinocytes. *Exp Cell Res* 313:1758–77

Choma DP, Milano V, Pumiglia KM, DiPersio CM (2007) Integrin alpha3beta1-dependent activation of FAK/Src regulates Rac1-mediated keratinocyte polarization on laminin-5. *J Invest Dermatol* 127:31–40

De Luca M, Pellegrini G, Zambruno G, Marchisio PC (1994) Role of integrins in cell adhesion and polarity in normal keratinocytes and human skin pathologies. *J Dermatol* 21:821–8

Deng M, Chen WL, Takatori A, Peng Z, Zhang L, Mongan M *et al.* (2006) A role for the mitogen-activated protein kinase kinase kinase 1 in epithelial wound healing. *Mol Biol Cell* 17:3446–55

Fitsialos G, Chassot AA, Turchi L, Dayem MA, LeBrigand K, Moreilhon C *et al.* (2007) Transcriptional signature of epidermal keratinocytes subjected to *in vitro* scratch wounding reveals selective roles for ERK1/2, p38, and phosphatidylinositol 3-kinase signaling pathways. *J Biol Chem* 282:15090–102

Franzke CW, Bruckner P, Bruckner-Tuderman L (2005) Collagenous transmembrane proteins: recent insights into biology and pathology. *J Biol Chem* 280:4005–8

Franzke CW, Tasanen K, Borradori L, Huotari V, Bruckner-Tuderman L (2004) Shedding of collagen XVII/BP180: structural motifs influence cleavage from cell surface. *J Biol Chem* 279:24521–9

Franzke CW, Tasanen K, Schacke H, Zhou Z, Tryggvason K, Mauch C *et al.* (2002) Transmembrane collagen XVII, an epithelial adhesion protein, is shed from the cell surface by ADAMs. *EMBO J* 21:5026–35

Friedl P (2004) Prespecification and plasticity: shifting mechanisms of cell migration. *Curr Opin Cell Biol* 16:14–23

Friedl P, Hegerfeldt Y, Tusch M (2004) Collective cell migration in morphogenesis and cancer. *Int J Dev Biol* 48:441–9

Huilaja L, Hurskainen T, Autio-Harmainen H, Hofmann SC, Sormunen R, Rasanen J *et al.* (2007) Pemphigoid gestationis autoantigen, transmembrane collagen XVII, promotes the migration of cytotrophoblastic cells of placenta and is a structural component of fetal membranes. *Matrix Biol* 27:190–200

Jablonska S, Fabjanska L, Milewski B (1958) Bullous diseases. II. Pemphigoid – its relation to pemphigus and Duhring's disease. *Przegl Dermatol* 8:609–20

Joubeh S, Mori O, Owaribe K, Hashimoto T (2003) Immunofluorescence analysis of the basement membrane zone components in human anagen hair follicles. *Exp Dermatol* 12:365–70

Labrousse AL, Buisson-Legendre N, Hornebeck W, Bernard P (2002) The metalloprotease-directed shedding of BP 180 (collagen XVII) from human keratinocytes in culture is unaffected by ceramide and cell-matrix interaction. *Eur J Dermatol* 12:240–6

Manohar A, Shome SG, Lamar J, Stirling L, Iyer V, Pumiglia K *et al.* (2004) Alpha 3 beta 1 integrin promotes keratinocyte cell survival through activation of a MEK/ERK signaling pathway. *J Cell Sci* 117:4043–54

Martin P, Parkhurst SM (2004) Parallels between tissue repair and embryo morphogenesis. *Development* 131:3021–34

McGrath JA, Gatalica B, Christiano AM, Li K, Owaribe K, McMillan JR *et al.* (1995) Mutations in the 180-kD bullous pemphigoid antigen (BPAG2), a hemidesmosomal transmembrane collagen (COL17A1), in generalized atrophic benign epidermolysis bullosa. *Nat Genet* 11:83–6

McGrath JA, Gatalica B, Li K, Dunnill MG, McMillan JR, Christiano AM *et al.* (1996) Compound heterozygosity for a dominant glycine substitution and a recessive internal duplication mutation in the type XVII collagen gene results in junctional epidermolysis bullosa and abnormal dentition. *Am J Pathol* 148:1787–96

McMillan JR, Akiyama M, Tanaka M, Yamamoto S, Goto M, Abe R *et al.* (2007) Small-diameter porous poly (epsilon-caprolactone) films enhance adhesion and growth of human cultured epidermal keratinocyte and dermal fibroblast cells. *Tissue Eng* 13:789–98

McMillan JR, McGrath JA, Tidman MJ, Eady RA (1998) Hemidesmosomes show abnormal association with the keratin filament network in junctional forms of epidermolysis bullosa. *J Invest Dermatol* 110:132–7

Messenger AG, Elliott K, Temple A, Randall VA (1991) Expression of basement membrane proteins and interstitial collagens in dermal papillae of human hair follicles. *J Invest Dermatol* 96:93–7

Nakamura H, Sawamura D, Goto M, Kida M, Ariga T, Sakiyama Y *et al.* (2006) Analysis of the COL17A1 in non-Herlitz junctional epidermolysis bullosa and amelogenesis imperfecta. *Int J Mol Med* 18:333–7

Nishie W, Sawamura D, Goto M, Ito K, Shibaki A, McMillan JR *et al.* (2007) Humanization of autoantigen. *Nat Med* 13:378–83

Osmanagic-Myers S, Gregor M, Walko G, Burgstaller G, Reipert S, Wiche G (2006) Plectin-controlled keratin cytoarchitecture affects MAP kinases involved in cellular stress response and migration. *J Cell Biol* 174:557–68

Parikka M, Nissinen L, Kainulainen T, Bruckner-Tuderman L, Salo T, Heino J *et al.* (2006) Collagen XVII promotes integrin-mediated squamous cell carcinoma transmigration-A novel role for alphaII(b) integrin and tirofiban. *Exp Cell Res* 312:1431–8

Pearson G, Robinson F, Beers Gibson T, Xu BE, Karandikar M, Berman K *et al.* (2001) Mitogen-activated protein (MAP) kinase pathways: regulation and physiological functions. *Endocr Rev* 22:153–83

Poumay Y, Roland IH, Leclercq-Smekens M, Leloup R (1994) Basal detachment of the epidermis using dispase: tissue spatial organization and fate of integrin alpha 6 beta 4 and hemidesmosomes. *J Invest Dermatol* 102:111–7

Pullikuth AK, Catling AD (2007) Scaffold mediated regulation of MAPK signaling and cytoskeletal dynamics: a perspective. *Cell Signal* 19:1621–32

Raja SK, Garcia MS, Isseroff RR (2007) Wound re-epithelialization: modulating keratinocyte migration in wound healing. *Front Biosci* 12:2849–68

Sams WM Jr (1970) Bullous pemphigoid. Is it an immunologic disease? *Arch Dermatol* 102:485–97

Schumann H, Baetge J, Tasanen K, Wojnarowska F, Schacke H, Zillikens D *et al.* (2000) The shed ectodomain of collagen XVII/BP180 is targeted by autoantibodies in different blistering skin diseases. *Am J Pathol* 156:685–95

Shimizu H, McDonald JN, Kennedy AR, Eady RAJ (1989) Demonstration of intra- and extra-cellular localization of bullous pemphigoid antigen using cryofixation and freeze substitution for postembedding immuno-electron microscopy. *Arch Dermatol Res* 281:443–8

Slack-Davis JK, Eblen ST, Zecevic M, Boerner SA, Tarcsafalvi A, Diaz HB *et al.* (2003) PAK1 phosphorylation of MEK1 regulates fibronectin-stimulated MAPK activation. *J Cell Biol* 162:281–91

Stoll SW, Kansra S, Elder JT (2003) Keratinocyte outgrowth from human skin explant cultures is dependent upon p38 signaling. *Wound Repair Regen* 11:346–53

Tasanen K, Tunggal L, Chometon G, Bruckner-Tuderman L, Aumailley M (2004) Keratinocytes from patients lacking collagen XVII display a migratory phenotype. *Am J Pathol* 164:2027–38

Zhang L, Koivisto L, Heino J, Uitto VJ (2004) Bacterial heat shock protein 60 may increase epithelial cell migration through activation of MAP kinases and inhibition of alpha6beta4 integrin expression. *Biochem Biophys Res Commun* 319:1088–95

Zillikens D, Giudice GJ (1999) BP180/type XVII collagen: its role in acquired and inherited disorders or the dermal-epidermal junction. *Arch Dermatol Res* 291:187–94

Zimina EP, Bruckner-Tuderman L, Franzke CW (2005) Shedding of collagen XVII ectodomain depends on plasma membrane microenvironment. *J Biol Chem* 280:34019–24

Zimina EP, Fritsch A, Schermer B, Bakulina AY, Bashkurov M, Benzing T *et al.* (2007) Extracellular phosphorylation of collagen XVII by ecto-casein kinase 2 inhibits ectodomain shedding. *J Biol Chem* 282:22737–46

In vivo far-red luminescence imaging of a biomarker based on BRET from *Cypridina* bioluminescence to an organic dye

Chun Wu[a], Kazuhiro Mino[b], Hidetoshi Akimoto[b], Makiko Kawabata[c], Koji Nakamura[c], Michitaka Ozaki[b], and Yoshihiro Ohmiya[a,b,d,1]

[a]Research Institute for Cell Engineering, National Institute of Advanced Industrial Science and Technology, 1-8-31 Midorigaoka, Ikeda 563-8577, Japan; [b]Graduate School of Medicine, Hokkaido University, Kita-15, Nishi-7, Kita-ku, Sapporo 060-8638, Japan; [c]LivTech, Inc, 907 Nogawa, Miyamae-ku, Kawasaki 216-0001, Japan; and [d]Research Institute for Genome-based Biofactory, National Institute of Advanced Industrial Science and Technology, 2-17-2-1 Tsukisamu-Higashi, Sapporo 062-8517, Japan

We aimed to develop a far-red luminescence imaging technology for visualization of disease specific antigens on cell surfaces in a living body. First, we conjugated a far-red fluorescent indocyanine derivative to biotinylated *Cypridina* luciferase. This conjugate produced a bimodal spectrum that has long-wavelength bioluminescence emission in the far-red region as a result of bioluminescence resonance energy transfer. To generate a far-red luminescent probe with targeting and imaging capabilities of tumors, we then linked this conjugate to an anti-human Dlk-1 monoclonal antibody via the biotin-avidin interaction. This far-red luminescent probe enabled us to obtain high-resolution microscopic images of live, Dlk-1-expressing Huh-7 cells without an external light source, and to monitor the accumulation of this probe in tumor-bearing mice. Thus this far-red luminescent probe is a convenient analytical tool for the evaluations of monoclonal antibody localization in a living body.

Cypridina luciferase | far-red luminescent probe | luciferin | tumor

An increasing number of monoclonal antibodies have been used to target antigens on cancer cells for clinical diagnosis and therapy, based on the fact that some antigens expressed on cancer cells surface reflect malignant behaviors invasion, metastasis, and neo-vascularization (1–5). Molecular imaging of antibodies in the whole body will enable us to prescribe the appropriate antibody therapy in terms of dose and the timing of administration. Fluorescence imaging (FLI) and bioluminescence imaging (BLI) have played an important role in molecular imaging in small animals (6–8). Photon detection is affordable and easy to use compared with radioisotope imaging. BLI is achieved with a luciferin-luciferase reaction in the presence of molecular oxygen. However, most bioluminescence spectra are in the visible region, overlapping with the absorption spectrum of hemoglobin, attenuating the bioluminescence intensity in live animals. Recently, a "self-illuminating quantum dot probe" was developed to improve the light penetration based on bioluminescence resonance energy transfer (BRET) between the bioluminescence of *Renilla* luciferase and quantum dots (9). The multivalent conjugation of *Renilla* luciferase to single dots allowed for highly efficient BRET between luciferase and quantum dots. However, the large size of the conjugate may cause problems in metabolism and localization in vivo (10).

BRET is a natural phenomenon observed in marine organisms. Green fluorescent protein, for example, is a well-known energy acceptor in the bioluminescence of *Renilla* luciferase and aequorin. BRET between the bioluminescence of *Renilla* luciferase and green fluorescent protein mutants has been used to study protein interactions (11). Recently several far-red fluorescent protein variants showing emission maxima around 650 nm were developed for in vivo imaging (12), but have not been well characterized as energy acceptors for BRET systems. On the other hand, the organic dyes indocyanine and its derivatives have molecular weights less than 1,200 Da, they produce far-red fluorescence and are widely used for in vivo imaging applications (13). Luciferase conjugated to such organic dyes is expected to create possibilities for in vivo applications.

Cypridina luciferase (CLuc) catalyzes the oxidation of *Cypridina* luciferin to yield light emission peaking at 460 nm (14). The luciferase genes from both the so-called sea fireflies *Cypridina* (*Vargula*) *hilgendorfii* and *C. noctiluca* have been cloned (15, 16); we used the latter. The 62-kDa CLuc has some unique properties as a bioluminescent enzyme (17). The secreted protein contains 17 disulfide bond pairs and is highly stable under physiological conditions. Its turnover rate (1,400 luciferin molecules per minute) is the highest among known luciferases (18). Recently we have established a method for the synthesis of the substrate, and have expressed the recombinant CLuc in yeast and applied it to ELISA (19, 20).

In the present study, we conjugated a far-red fluorescent indocyanine derivative to biotinylated CLuc via glycol-chains and named this far-red bioluminescent protein "FBP." A monoclonal antibody against human Delta-like protein (Dlk-1), one of the embryonic antigens expressed on the surface of many cancer cells, was then produced (21–25). Using anti-Dlk-1 monoclonal antibody linked to FBP via biotin-avidin interaction, we achieved bioluminescence imaging of cancer cells in vivo as well as in vitro.

Results

We designed FBP based on BRET (Fig. 1A). To obtain biotinylated CLuc (*SI Text*), we attached an Avi-Tag consisting of a 16-residue peptide SGLNDIFEAQKIEWHE to the C terminus of CLuc (26). We then conjugated biotinylated CLuc with the indocyanine derivative HiLyte Fluor™ 647 hydrazide via the glycol-chains of CLuc. The band of FBP on SDS/PAGE was shifted to high molecular weight compared with that of biotinylated CLuc (Fig. 1B, lanes 1 and 2). The average substitution was estimated to be two dyes per CLuc molecule from the UV absorption spectrum.

FBP showed a bimodal bioluminescence spectrum, attributable to intra-molecular BRET, having emission peaks at 460 nm and at 675 nm. To investigate the possible effect of pH and ion concentration, we measured bioluminescence spectra under different conditions. No appreciable change was observed (Fig.
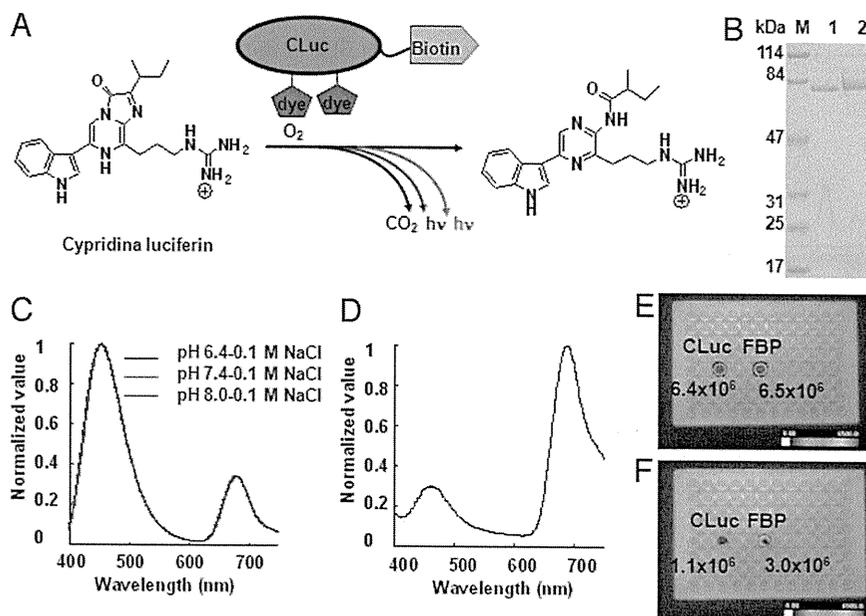
Fig. 1. (A) Schematic of FBP and its bioluminescence reaction. (B) SDS/PAGE of biotinylated CLuc (lane 1) and FBP (lane 2). (C) Bioluminescence spectra of FBP measured in different pH buffer solutions containing 0.1 M NaCl. Curves all superimpose. (D) Bioluminescence spectrum of FBP in blood. (E) Relative light intensity of FBP or CLuc in buffer. (F) Relative light intensity of FBP or CLuc in blood.

1C and Fig. S1), indicating that the BRET signal was constant under different physiological conditions. To examine whether the BRET signal could be detected in vivo, we measured the bioluminescence spectrum of FBP in mouse blood (Fig. 1D). The far-red emission peak was dominant in the bioluminescence spectrum. Furthermore, to compare light intensity of FBP and CLuc under various conditions, we measured these probes in buffer as well as in blood with a commercial CCD imaging system. We found the light intensity of FBP was almost the same as that of CLuc in buffer (Fig. 1E), whereas the light intensity of FBP in blood was three-times higher than that of CLuc (Fig. 1F). These results suggested that FBP is suitable for in vivo imaging in live animals.

Dlk-1 is one of the embryonic antigens expressed on the surface of many cancer cells. It is highly expressed in fetal tissues including liver, but is undetectable in adult liver (23). To obtain a monoclonal antibody against Dlk-1, we prepared a human embryonic kidney cell line (HEK293 cells) stably expressing Dlk-1-antigen (HEK293-Dlk-1). Mice (BALB/c) were immunized with HEK293-Dlk-1cells or with the expression vector that encodes full-length Dlk-1 cDNA. An anti-human Dlk-1 monoclonal antibody (DI-2–20) was screened by ELISA and flow cytometry. Immunocytochemical analyses showed that the anti-human Dlk-1 monoclonal antibody detected Dlk-1 antigen on Dlk-1-positive human hepato-cellular carcinoma cell line (Huh-7 cells) (Fig. 2A). In contrast, no green fluorescence signal was found on the surface of Dlk-1-negative Huh-7 cells (Fig. 2B). Western blot analyses clearly indicated the exclusive expression of Dlk-1 antigen on Dlk-1-positive Huh-7 cells (Fig. 2C).

After the antibody was conjugated to maleimide-activated avidin, we loaded the reaction mixture on a size-exclusion column (Fig. 3A). The eluted fractions were subjected to a bioluminescence ELISA using FBP and anti-mouse IgG coating plate. A high molecular weight protein of approximately 500 kDa showed strong bioluminescence (Fig. 3B). To reduce the size of the antibody and avidin conjugate, we treated the antibody with 2-mercaptoethylamine, a mild reducing agent that can selectively cleave hinge-region disulfide bonds between the heavy chains of antibody molecules. The two functional half antibodies were then conjugated to maleimide-activated avidin and purified on

a size-exclusion column (Fig. 3C); the reduced antibody-avidin conjugate of approximately 200 kDa was collected (Fig. 3D).

To evaluate the capabilities of the far-red luminescent probe, which we now call FBP-IgG, consisting of FBP and avidin-bound antibody (Fig. 4A), we performed microscopic BLI. After incubating the conjugate with Dlk-1-positive or Dlk-1-negative Huh-7 cells cultured in a dish, a strong bioluminescence signal was observed from Dlk-1-positive Huh-7 cells, but not from Dlk-1-negative Huh-7 cells (Fig. 4 B and C). For comparison, we similarly prepared a probe CLuc-IgG by mixing biotin-CLuc with avidin-bound reduced anti-Dlk IgG.
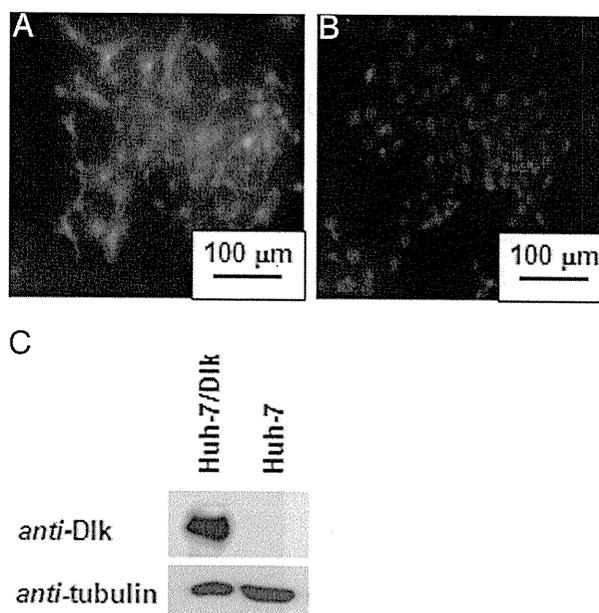

Fig. 2. Dlk-1-positive Huh-7 cells. (A and B) Fluorescence micrographs of Dlk-positive Huh-7/Dlk-1 cells and Huh-7 cells. Hoechst33342 and FITC were used for nuclear staining (blue) and Dlk-1 staining (green), respectively. (C) Western blot analyses of Dlk-1-positive and Dlk-1-negative Huh-7 cells.